Molecular Immunology 111 (2019) 182–197

Contents lists available at ScienceDirect

Molecular Immunology

journal homepage: www.elsevier.com/locate/molimm

Immunogenicity and protective efficacy of mucosal delivery of recombinant hcp of *Campylobacter jejuni* Type VI secretion system (T6SS) in chickens

Ankita Singh, Khairun Nisaa, Sudipta Bhattacharyya, Amirul Islam Mallick*

Department of Biological Sciences, Indian Institute of Science Education and Research Kolkata, Mohanpur, Nadia, West Bengal, 741246, India

ARTICLE INFO

Keywords:
Campylobacter jejuni
Chickens
Hemolysin co-regulated protein
Chitosan nanoparticles
Mucosal immunity

ABSTRACT

The type VI secretion system (T6SS) has recently emerged as a new pattern of protein secretions in *Campylobacter jejuni (C. jejuni)*. Within the T6SS cluster, hemolysin co-regulated protein (hcp) is considered as a hallmark of functional T6SS and holds key role in bacterial virulence. As poultry is the primary reservoir of *C. jejuni* and the major sources for human infection, we evaluated the capacity of recombinant hcp (rhcp) immunization in blocking *C. jejuni* colonization in chickens with an aim to control bacterial transmission to humans via poultry food chain. Considering the mucosal route is the primary portal for *C. jejuni* entry and gut mucosa offers the apposite site for *C. jejuni* adherence, we investigated the immune-protective potential of intra-gastric administration of rhcp using chitosan-based nanoparticles. To achieve this goal, full length coding sequence of hcp gene from *C. jejuni* was cloned and expressed in *E. coli*. Purified rhcp was entrapped in chitosan-Sodium tripolyphosphate nanoparticles (CS-TPP NPs) and orally gavaged in chickens. Our results suggest that intra-gastric immunization of CS-TPP-rhcp induces consistent and steady increase in intestinal (sIgA) and systemic antibody (IgY) response against rhcp with significant reduction in cecal load of *C. jejuni*. The protection afforded by rhcp associated cellular responses with Th1 and Th17 profile in terms of increased expression of NFkB, IL-1β, IL-8, IL-6, IFN-γ and IL-17 A genes. Though systemic immunization of rhcp with IFA resulting in a robust systemic (IgY) and local (sIgA) antibody response, mucosal administration of rhcp loaded CS-TPP NPs was found to be superior in terms of bacterial clearance. Altogether, present study suggests that chitosan based intra-gastric delivery of rhcp have several advantages over the injectable composition and could be a promising vaccine approach to effectively control *C. jejuni* colonization in chickens.

1. Introduction

The type VI secretion system (T6SS) has emerged as an important virulence mechanism in number of Gram negative bacteria (Basler and Mekalanos, 2012; Basler et al., 2012; Leiman et al., 2009; Pukatzki et al., 2006). Its role in bacterial export pathway with a capacity to translocate effectors molecules into diverse targets has been well studied in *Pseudomonas aeruginosa*, *Vibrio cholerae*, *Escherichia coli*, *Burkholderia thailandensis*, *Serratia marcescens*, *Burkholderia mallei* and *Salmonella enterica* (Dudley et al., 2006; Mougous et al., 2006; Murdoch et al., 2011; Parsons and Heffron, 2005; Pukatzki et al., 2006; Schell et al., 2007; Schwarz et al., 2010). Recently the presence of T6SS in *Campylobacter jejuni* (*C. jejuni*) has been reported and its possible contribution in host pathogenicity, bacterial survival or evasion of immune defence has been proposed in the light of analogous function seen in the case of other bacteria (Lertpiriyapong et al., 2012; Lien and Lai, 2017).

Bacterial T6SS resembles an inverted phage like-puncturing device, composed of 13 core proteins, TssA to M, which are generally encoded by a group of tightly clustered genes (Boyer et al., 2009; Silverman et al., 2012). Among them hemolysin co-regulated protein (hcp or TssD) is considered as a hallmark for functional T6SS and often detected in the culture supernatant of the major Gram negative bacteria with functional T6SS (Mougous et al., 2006; Wu et al., 2008; Zhou et al., 2012). Previously, the role of hcp was demonstrated to have direct correlation with bacterial pathogenesis and its self-survival in case of *V. cholerae*. Successive studies further suggested the immunogenic potential of recombinant hcp of *B. pseudomallei* and proved to be protective in mice (Burtnick et al., 2011). While the role of anti-hcp host response to prevent bacterial survival, cell adhesion was explored in the past against other gut pathogens, however, to our knowledge the use of hcp as a core component of *C. jejuni* functional T6SS in the light of a prospective vaccine candidate has never been tested. Since T6SS from majority of the Gram negative bacteria possess identical structure with extensive protein homology, the benefit of a vaccine composed of

* Corresponding author.
E-mail address: amallick@iiserkol.ac.in (A.I. Mallick).

https://doi.org/10.1016/j.molimm.2019.04.016
Received 25 July 2018; Received in revised form 5 February 2019; Accepted 23 April 2019
Available online 09 May 2019
0161-5890/ © 2019 Elsevier Ltd. All rights reserved.

conserved and functional component of T6SS, such as hcp, could be beneficial for the host protection against wide range of Gram negative bacteria expressing immunologically related T6SS.

Because the naturally acquired *C. jejuni* has little or no pathogenic outcome in case of chickens, considering the risk associated with *C. jejuni* transmission to human via contaminated poultry and poultry products, the need for an effective vaccine to reduce the *C. jejuni* colonization in chickens is very important (Connell et al., 2012; Hermans et al., 2012; Newell and Fearnley, 2003; Sahin et al., 2002). To this end, the present research investigated the potential benefits of mucosal immunization of recombinant hcp (rhcp) of *C. jejuni* using Chitosan (CS) based nanoparticles (NPs) in inducing protective immune response required for blocking *C. jejuni* colonization in chickens gut. Owing to the several advantages exhibited by chitosan including biocompatibility, biodegradability, low immunogenicity we specifically chose to use CS-based NPs with an anticipation that intra-gastric delivery of rhcp via CS NPs would protect the antigen during gut transit and activate local immune response (Agnihotri et al., 2004; Pandey et al., 2005; Plapied et al., 2010; Sayin et al., 2009). Here we provide direct evidence that intra-gastric administration of rhcp entrapped in Chitosan-Sodium tripolyphosphate nanoparticles (CS-TPP NPs) effectively reduce the bacterial load in ceca when challenged with hypervirulent *C. jejuni* isolate. Our result demonstrating the value of mucosal immunization over systemic mode in blocking *C. jejuni* colonization in chickens further suggests the advantages of CS based NPs as a safer alternative to adjuvanted injectable vaccine as the latter is known to slow down the growth of the birds due to adjuvant or carrier deposition in soft tissues.

In addition to significant elevation of local antibody response (sIgA) in the intestine, we showed that mucosal delivery of rhcp could substantially improve the systemic antibody (IgY) responses in chickens. However, despite the fact that intestinal antibody (sIgA) plays key role in blocking of *C. jejuni* adherence and subsequent reduction in enteric colonization in chickens, the precise roles of serum antibody in contributing functional immunity to C. jejuni remain unclear (Layton et al., 2011). Except at early post hatch time points when maternal antibodies (mIgY) afford effective protection against bacterial colonization, immune clearance of *C. jejuni* by serum IgY is, in fact, slow (Lacharme-Lora et al., 2017; Sahin et al., 2003; Thibodeau et al., 2017). Consequently, naturally acquired *C. jejuni* when inhabit the ceca, the growing birds become an important source for bacterial transmission to human.

It was of our interest to see whether the robust local or systemic antibody response could facilitate activation of its cellular counterpart following oral immunization with rhcp. We observed a significant up-regulation of Th1 and Th17 transcriptional profile in terms of increased expression of NFkB, IL-1β, IL-8, IL-6, IFN-γ and IL-17 A genes in splenic tissue.

Given that adherence of intestinal cells by *C. jejuni* is the key reason for enteric colonization in chickens, collectively the present study suggests the potential of intra-gastric delivery of rhcp as an effective mucosal vaccine strategy against *C. jejuni* in chickens.

2. Materials and methods

2.1. Bacterial strains, vectors,cell lines, growth conditions and other reagents

C. jejuni (*BCH71*) isolated from clinical human samples were kindly provided by Dr. Ashish Mukhopadhyay, Scientist "E", NICED (ICMR) Kolkata, West Bengal, India and maintained in our laboratory as per standard methods (L. Davis and DiRita, 2008). Briefly, *C. jejuni* isolates were grown in Mueller Hinton broth in presence of CAT supplement for 48 h at 37 °C under microaerophilic condition (10% CO_2, 5% O_2 and 85% N_2) using microaerophilic generating gas pack (Anaerogas pack 3.5 L, HiMedia, India). *E. coli* DH5α strain (Life Technology, USA) was used as cloning host while *E. coli* M15 [pREP4] (Qiagen, USA) cells were used as expression host. pMD20 vector (TaKaRa, Japan) and prokaryotic pQE30 vector (Qiagen, Inc., USA) were used for gene cloning and expression study respectively. Recombinant plasmids were maintained in *E. coli* DH5α and M15 cells and grown under antibiotic selection using ampicillin 50 μg/ml and kanamycin 20 μg/ml respectively, whenever needed.

Chemicals and reagents used in this study was of highest purity available. Chitosan (CS) was purchased from HiMedia Laboratory (India) and Sodium Tripolyphosphate (TPP) was procured from Loba Chemie (India). Bicinchoninic acid (BCA) protein assay kit was procured from Pierce Chemical Co., (USA). Incomplete Freund's Adjuvant was obtained from Sigma (USA). Mouse monoclonal anti-His antibody, HRP conjugated anti-mouse IgG (H + L) antibody were purchased from Thermo Fisher Scientific (USA) while anti-chicken IgY (HRP) and anti-chicken IgA (α chain; HRP) antibody were procured from Abcam (UK) and Bethyl Laboratories (USA) respectively. Goat anti-rabbit IgG (HRP) antibody was obtained from BioBharati (India). Enzyme substrate 3, 3′, 5, 5′-tetramethyl benzidine (TMB), 3,3-Diaminobenzidine, Luria Bertani media (LB), Mueller Hinton (MH) broth, Blood Free Campylobacter Selectivity Agar Base Media, CAT selective supplement (cefoperazone 8 mg/L, amphotericin 10 mg/L, and teicoplanin 4 mg/L) were obtained from HiMedia. All the primers used in this study were synthesized by IDT technologies (USA) and listed in Table 1. Cell lines (INT407 and Caco-2) used in this study were purchased from NCCS, Pune (India) and maintained in our lab as per the standard protocol while primary chicken embryo intestinal cells (CEICs) were prepared as per the method described previously (Singh and Mallick, 2019).

Table 1
List of the primers used in this study.

S.No.	Target genes	Primer sequences	Amplicon size (bp)	Ref.
1	hcp	F- 5' TGGCTGAACCAGCGTTTATAAAAATTG 3' R- 5' TTAAGCTTTGCCCTCTCTCCA 3'	510	This study
2	β-actin	F- 5' GAGAAATTGTGCGTGACATCA 3' R-5' CCTGAACCTCTCATTGCCA 3'	152	(Li et al., 2008)
3	NFkB	F- 5' GAAGGAATCGTACCGGGAACA 3' R- 5' CTCAGAGGGCCTTGTGACAGTAA 3'	131	(Chiang et al., 2009)
4	IL-1β	F- 5' TGGGCATCAAGGGCTACA 3' R- 5' TCGGGTTGGTTGGTGATG 3'	244	(Hong et al., 2006)
5	IL-8	F- 5' GGCTTGCTAGGGGAAATGA 3' R- 5' AGCTGACTCTGACTAGGAAACTGT 3'	200	(Hong et al., 2006)
6	IL-6	F- 5' GGAACAACCTCAACCTGCCCAAGG 3' R- 5' CCAGGTGCTTTGTGCTGTAGCAC 3'	310	This study
7	IFN-γ	F-5' ACACTGACAAGTCAAAGCCGCACA 3' R-5' AGTCGTTCATCGGGAGCTTGGC 3'	129	(Mallick et al., 2011)
8	IL-17 A	F- 5' ATTCCAGGTGCGTGAACTCGGC 3' R- 5' GTGCAGCCCACGGTGATCATTTTC 3'	148	This study

2.2. Cloning of hcp gene ofC. jejuniisolated from clinical human sample

To clone hcp gene, genomic DNA was extracted from *C. jejuni* (*BCH71*) of human origin as per the standard protocol (Chen and Kuo, 1993). Full length coding sequence of hcp gene was next amplified by PCR using the following primer pair: Forward 5′ CCGCGGTACCATGG CTGAACCAGCGTTTATAAAAATTG 3′; Reverse: 5′ GACTACTGCAGTT AAGCTTTGCCCTCTCTCCA 3′. The 5′ ends of the forward and reverse primers contained *Kpn*I and *Pst*I restriction sites (underlined), respectively. Amplified hcp gene was then directly cloned into pMD20 cloning vector and transformed into *E. coli* DH5α competent cells. Positive transformants were screened and sequence analysed. In order to express rhcp, PCR amplified product from pMD20-hcp recombinant plasmid was sub-cloned into the pQE30 expression vector in the C terminal of a hexa-histidine sequence (6xHis) using above mentioned primer sets. The ligated recombinant plasmid was transformed into *E. coli* M15 cells and positive colonies were screened by colony PCR.

2.3. Expression and purification of rhcp

To express the recombinant protein, *E. coli* M15 cells having recombinant plasmid were grown in LB broth containing ampicillin 50 μg/ml and kanamycin 20 μg/ml. When the optical density (OD_{600}) reached 0.5 protein expression was induced with β-D isopropyl thiogalactopyranoside (IPTG) at a final concentration of 1 mM and incubated for additional 5 h at 37 °C. The induced cells were pelleted by centrifugation at 5000 *g* for 20 min at 4 °C and resuspended in lysis buffer (pH 8.0) containing 50 mM NaH_2PO_4, 300 mM NaCl, 10 mM Imidazole and 1 mM Protease inhibitor (PMSF, HiMedia) followed by sonication for 30 min. Finally, the supernatant of the bacterial cell lysate containing released protein was collected by centrifugation at 4000 *g* for 20 min and loaded to gravity column having Ni^{2+}-NTA agarose beads (Qiagen, USA) that had been pre-equilibrated with binding buffer. Further purification process was performed following manufacturer's instruction (Qiagen). The bound protein eluted with elution buffer (50 mM NaH_2PO_4, 300 mM NaCl, 250 mM Imidazole, pH 8.0) was dialyzed against PBS (pH 7.4) and the concentration of the recombinant protein was measured by BCA method. The size and purity of the recombinant protein was further confirmed by SDS-PAGE analysis followed by Western blot as per the method described elsewhere with slight modification (Nothaft et al., 2016). Briefly, hexa-histidine tagged rhcp was probed with mouse monoclonal anti-His primary antibody followed by immune-labelling with HRP conjugated Goat anti-mouse IgG (H + L) secondary antibody. The immunoblot was visualized using ECL western blotting substrate (Promega, USA).

2.4. Cytotoxicity of rhcp in human and chicken cells

To determine the cell cytotoxicity of rhcp, 50% cytotoxic concentration (CT_{50}) was determined in both polarized (Caco-2) and non-polarized human cell lines (INT407) as well as in chicken CEICs using MTT assay as per the method described previously with minor modifications (Jafarlou et al., 2016). In brief, 6×10^3 cells/well were seeded in 96-well tissue culture plates for 48 h at 37 °C under 5% CO_2 pressure. Confluent monolayers of cells were treated with different concentration of rhcp ranging from 0.1 μg/ml to 30 μg/ml and incubated for 24 h. Following incubation, cells were washed with PBS and replaced with fresh complete media. Finally, to each well 10 μl of MTT dye dissolved in PBS (1 mg/ml) was added and incubated for another 3 h at 37 °C under 5% CO_2 pressure. The water insoluble formazan crystals thus formed was solubilized with dimethyl sulphoxide (DMSO) (100 μl/well) and the absorbance was measured at 595 nm using microplate reader (BioTek). The 50% cytotoxic concentration (CT_{50}) with respect to untreated control (cells with media only) was calculated by using nonlinear regression in GraphPad Prism software. The CT_{50} values calculated from MTT assay were further verified by Sulphorhodamine B assay (SRB assay) under similar condition. Details of the methodology is described in the supplementary materials (Supplementary Section S2).

2.5. Comparative assessment of the immunoreactivity of recombinant as well as native hcp

To assess the immunoreactivity of *E. coli* expressed rhcp, polyclonal antibodies were raised in New Zealand White rabbit against the purified rhcp according to the protocol described previously with slight modification (Bleumink-Pluym et al., 2013). Briefly, 150 μg of purified rhcp emulsified with incomplete Freund's adjuvant (IFA) was injected through subcutaneous route. Rabbit was given booster dose twice at weekly interval with half the previous amount of protein. Blood was collected from the ear vein on day 7 post last immunization. Serum aliquots were kept at - 20 °C till further use. A schematic representation of immunization regimen is provided in (Fig. 3; Panel A).

Since *E. coli* M15 cells lack glycosylation machinery, we further test the ability of the anti-rhcp antibody in recognition of native hcp expressed by a *C. jejuni* isolate harbouring functional T6SS including hcp gene by indirect ELISA. Details of the methodology is described in the supplementary materials (Supplementary Section S1).

2.6. Immunogen preparation

2.6.1. Preparation of chitosan-based nanoparticles

To deliver rhcp through mucosal route, nanoparticles (NPs) composed of chitosan (CS) cross-linked with Sodium tripolyphosphate (TPP) were prepared following published protocol (Sawaengsak et al., 2014). Briefly, 0.5% (w/v) CS stock solution was prepared by dissolving dried CS powder in 1% aqueous acetic acid (v/v) and mixed properly until a transparent solution was obtained. A working solution of CS (0.05%) and TPP (0.1%) were prepared by diluting the stock solution with 25 mM sodium acetate buffer (pH 5.4) and ultrapure distilled water respectively. Next, CS was cross-linked by adding TPP (3:1 v/v) and incubated at 25 °C for 2 h under continuous stirring followed by centrifugation at 14,000 *g* for 20 min to obtain the slurry containing desired NPs.

2.6.2. Entrapment of rhcp into CS-TPP NPs

Recombinant hcp was encapsulated into CS-TPP NPs as per the protocol described previously (Sawaengsak et al., 2014). Briefly, 700 μl of protein solution containing 70 μg of purified rhcp was mixed with 3.3 ml of CS solution followed by dropwise addition of 1 ml of TPP solution. The mixture was stirred for 2 h at 25 °C. The slurry formed was pelleted by centrifugation at 14,000 *g* for 20 min and resuspended in 0.5 ml sterile PBS (pH 7.4). The entrapment efficiency (EE) was calculated as the percentage of protein retained by the CS-TPP NPs using the following equation:

$$\text{Entrapment efficiency (EE)} = [(rhcp_{total} - rhcp_{sup})/\ rhcp_{total}] \times 100.$$

where, $rhcp_{total}$ is the total amount of rhcp added during the formation of CS-TPP NPs and $rhcp_{sup}$ is the amount of rhcp present in the supernatant (unentrapped).

2.7. Physiochemical characterization of rhcp loaded CS-TPP NPs

2.7.1. FT-IR analysis

To confirm the formation of cross-linking between CS and TPP, IR spectroscopy of formed NPs was performed as per the method described previously with slight modification (Rashid et al., 2015). In brief, NPs either in free form or loaded with rhcp were vacuum dried and mixed with potassium bromide (KBr). FT-IR spectrum of the prepared sample was recorded using PerkinElmer Spectrum Two™ FT-IR spectrometer in

the operating range of 4000–400 cm^{-1} at a resolution of 4 cm^{-1}. Data was corrected against baseline obtained using blank KBr pellets. For comparative analysis, data was also recorded for free CS and TPP separately.

2.7.2. Dynamic light scattering (DLS) and measurement of zeta potential (ζ)

The hydrodynamic radii, size distribution, surface charge (zeta potential; ζ) and polydispersity index (PDI) of CS-TPP NPs before and after loading with rhcp were determined as described previously with minor changes (Al-Manasir et al., 2009; Schrøder et al., 2014). In brief, free and rhcp encapsulated NPs were diluted in milliQ water (1:10) and sonicated for 10 min. The samples were then analysed for size distribution using DLS and surface charge by laser doppler micro-electrophoresis respectively using Malvern Zetasizer Nano ZS instrument (USA). The measurement was performed in triplicate using water as solvent at 25 °C.

2.7.3. Scanning electron microscopy (SEM) analysis

External morphology of the synthesised CS-TPP NPs were investigated through analyses of SEM image (Carl Zeiss SUPRA 55 V P FESEM). Sample for SEM was prepared following procedure as described elsewhere with minor modification (Kamat et al., 2015). Briefly, following dispersion of the NPs in milliQ water (1:10), the sample was sonicated for 30 min in a bath type sonicator (Thermo Fisher Scientific, USA) and drop casted on glass coverslips. Samples were thoroughly dried under vacuum desiccator. Before scanning, the samples were sputter-coated with a thin layer of gold for allowing SEM visualisation (as the samples are non-conducting). The particle diameters were calculated by post image analysis using ImageJ software (USA) after calibration.

2.7.4. Transmission electron microscopy (TEM)

For TEM analysis of CS-TPP NPs, samples were diluted (1:100) in milliQ water and sonicated for 30 min. Approximately 7 µl of this diluted suspension was added to 300-mesh formvar carbon coated copper grids (Electron Microscopy Sciences, UK) and stained with UranyLess (Electron Microscopy Sciences) as negative staining following manufacturer's protocol. Samples were drop casted over the grids and left undisturbed for 30 min, extra fluid was removed with filter paper and air dried for overnight under vacuum. Data acquisition was performed using JEOL JEM-2100 Plus LaB_6 series electron microscope (Japan) operating at an accelerating voltage of 120 kV. Both high and low-resolution images were captured and were analysed using ImageJ software.

2.7.5. In vitro release kinetics of rhcp from CS-TPP NPs

In vitro release profile of entrapped rhcp in two different conditions (varied pH and buffer composition) was assessed as per the methods described previously with some modification (Abkar et al., 2017). Briefly, the *in vitro* release assay of rhcp was performed in phosphate buffered saline (PBS; pH 7.4) and simulated gastric fluid (SGF; 2 g NaCl and 7 ml HCl in 1 L of water; pH 1.2). In brief accurately weighed pellet containing rhcp loaded CS-TPP NPs were thoroughly washed in PBS to remove unbound proteins by centrifugation at 14,000 *g* for 20 min at 4 °C followed by resuspending in 0.2 ml PBS and SGF separately. The suspension was incubated at 42 °C under continuous agitation by means of stirring (150 rpm) and supernatant containing released protein was collected at different time intervals by centrifuging the suspension at 14,000 *g* for 10 min. At each time point, equal amount of fresh buffer was replaced by adding either PBS or SGF. The concentration of rhcp present in the supernatant was determined at wavelength 280 nm based on molar extinction co-efficient (21,033 cm^{-1} M^{-1}) and molecular weight of hcp using Nanodrop TM 2000c Spectrophotometer (Thermo Fisher Scientific, USA). The fraction released of rhcp was calculated as per the following equation:

$$\text{Fraction released (\%)} = [rhcp_{sup} / rhcp_{ent}] \times 100$$

where, $rhcp_{sup}$ is the amount of rhcp measured in the supernatant and $rhcp_{ent}$ is the amount of rhcp entrapped in the NPs.

2.7.6. Structural and functional analysis of released rhcp from CS-TPP NPs

2.7.6.1. Protein integrity and western blot detection. To confirm the integrity of entrapped as well as released rhcp, SDS-PAGE and Western blot analysis were performed. For protein integrity of entrapped rhcp, CS-TPP NPs were destabilized with 10% (w/v) NaCl and was subjected to 15% SDS-PAGE as per the method described previously (Abkar et al., 2017). Further, the specific recognition of released rhcp was assessed by Western blot using mouse monoclonal anti-His antibody as well as rabbit polyclonal anti-rhcp antibody as per the method described in section 2.3.

2.7.6.2. Circular dichroism (CD) analysis. To study the structural conformation, protein's secondary structure was verified at pH 8.0 [Tris buffer (20 mM Tris-HCl; 150 mM NaCl)] and 1.2 (SGF buffer) by CD using JACSO-1000 spectropolarimeter (USA). Briefly, rhcp was dialysed against Tris buffer (pH 8.0) and SGF (pH 1.2) separately. Recombinant hcp in Tris buffer was run as control. Similarly, released rhcp was thoroughly centrifuged to remove the residual NPs and dialysed against SGF. Finally, 250 µg of dialysed rhcp and released rhcp were subjected for CD analysis. The CD signal in the range from 190 nm to 300 nm was monitored using a thermostatic (25 °C) with a quartz cuvette (1 mm path length). Baseline correction was performed using respective dialysis buffer and data acquisition was performed in triplicate. Finally, the CD spectral matching of rhcp as well as released rhcp was performed after smoothing using polynomial order 2 (10 data point smoothing).

2.7.6.3. Cytotoxicity of released rhcp. For functional analysis, cell cytotoxicity of released rhcp from CS-TPP NPs using human INT407, Caco-2 and chicken CEICs was evaluated by MTT and SRB assays as per the methods described in section 2.4.

2.8. In vivo chicken experimentation

2.8.1. Experimental chickens and immunization

A total of 40 day-old Vencobb chicks were received from The Venky's Hatcheries, AP (India) and placed into standard housing system. Chicks were given antibiotic-free diet *ad libitum* and water. Birds were fed with a standard starter diet up to 14 days of age and then received a grower diet until the end of the experiment. The *in vivo* experiment was repeated three times under similar condition.

At day 7 all the birds were randomly divided into four groups (n = 10 for each experiment) and received three consecutive treatments at one-week interval. A schematic representation of immunization regiment is presented in (Fig. 9; Panel A). The experimental groups were maintained as: Group 1: PBS; Group 2: Sham CS-TPP NPs (no antigen); Group 3: rhcp loaded CS-TPP NPs (CS-TPP-rhcp) and Group 4: rhcp with Incomplete Freund's adjuvant (IFA-rhcp). Each bird belonging to the Group 1 to 3 were orally gavaged with 200 µl of PBS, Sham CS-TPP NPs and CS-TPP NPs loaded with ~50 µg of rhcp respectively. Birds belonging to the Group 4 received subcutaneous injection of 100 µl of ~50 µg of rhcp emulsified with IFA. Each group received two booster immunization at day 14 and day 21 with half of the amount of rhcp used for primary immunization. At day 7 post last immunization half of the birds from each group were sacrificed by cervical dislocation.

2.8.2. Sample collection

Serum and faeces: Blood and fresh cloacal faeces were collected from each bird at weekly interval throughout the experiment. Serum

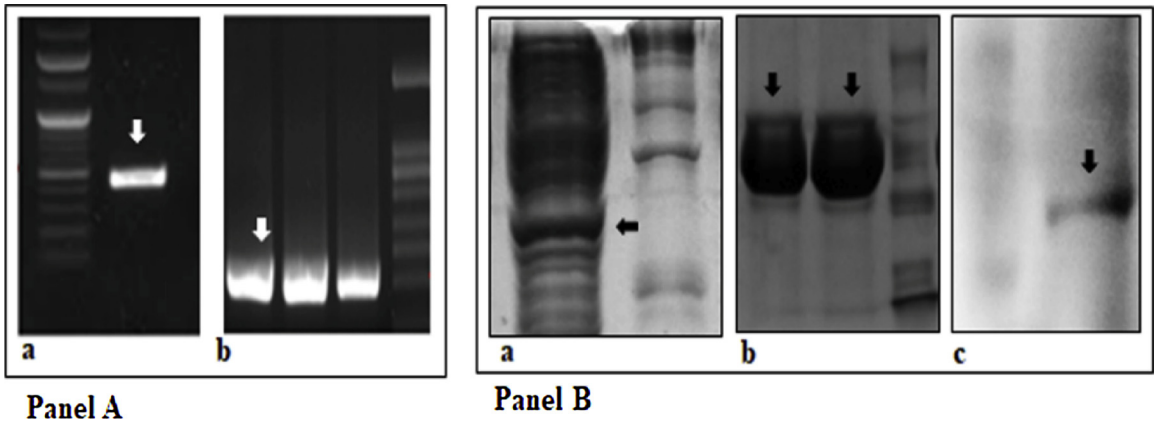

Fig. 1. Cloning and expression of rhcp gene of *C. jejuni* isolated from human clinical samples.
Panel A: Genomic DNA of *C. jejuni* isolated from human clinical samples were used as template to amplify hcp gene of T6SS cluster (a). A 510 bp product corresponding to the size hcp gene was purified, digested and cloned into a prokaryotic expression vector (pQE30). Colony PCR of positive transformant of *E. coli* M15 cells showing expected size of gene product (b). Panel B: SDS-PAGE analysis of IPTG induced recombinant *E. coli* M15 cells showing expression of hcp at ~ 20 kDa position (a). Integrity and purity of the affinity column purified rhcp was confirmed by SDS-PAGE (b). Western blot analysis affirmed the recognition of hexa-histidine tagged rhcp at the expected size (c).

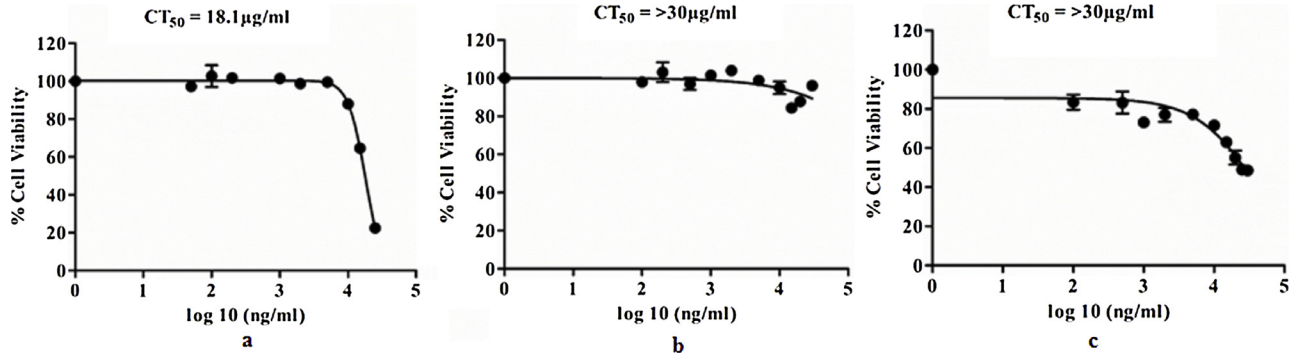

Fig. 2. Cytotoxicity of rhcp in human INT407, Caco-2 and primary chicken embryo intestinal cells (CEICs) by MTT assay.
Cytotoxic effect of rhcp in INT407 (a), Caco-2 (b) and CEICs (c). Cells were treated with rhcp ranging from 0.1 µg/ml to 30 µg/ml for 24 h. Next, the cells were thoroughly washed and incubated with 10 µL of MTT solution (1 mg/ml) for 3 h. Following incubation cells were dissolved in DMSO and the absorbance was read at 595 nm. CT_{50} value of rhcp was determined to be 18.1 µg/ml for INT407 whereas for Caco-2 and CEICs, CT_{50} values were found to be > 30 µg/ml. Each data point represent the mean of cell viability ± SE relative to the untreated cells normalized to 100% of two independent experiments in quadruplicate.

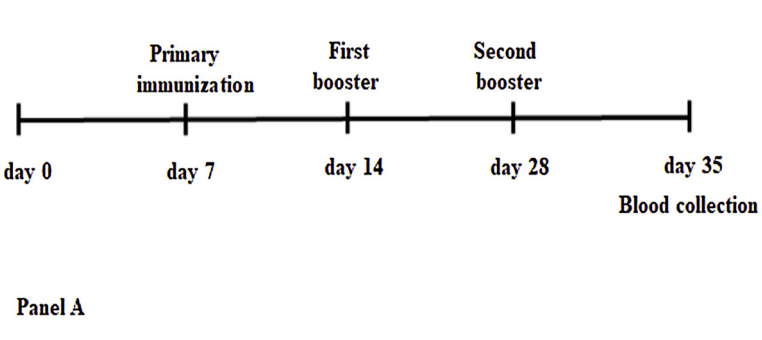

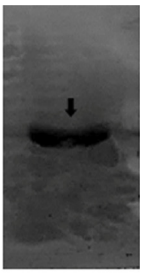

Fig. 3. Raising rabbit polyclonal hyperimmune sera against rhcp and Western blot analysis. Schematic representation of rabbit immunization regimen using rhcp emulsified in IFA (Panel A).
Western blot analysis of rhcp probed with hyperimmune rabbit polyclonal sera (1:1000 dilution) confirmed the immunoreactivity and specificity of the immunizing protein. Immunoblot is indicated with arrow (Panel B).

was separated, aliquoted and stored at -20 °C till further use. Freshly collected cloacal faeces (0.5 g) were processed as per the method described previously and stored at -20 °C (Maciel et al., 2004).

Tissue samples: Approximately 70 g of spleen from each bird were collected at day 7 post last immunization (before challenge) and stored in RNA later (Qiagen, USA) at −20 °C.

Intestinal lavage: Intestinal lavages were harvested and processed as per the standard method published elsewhere with slight modification (Suarez et al., 2010). Briefly, intestinal lavage was collected from ileo-cecum junction in 0.8 ml PBS and centrifuged at 1000 *g* for 10 min. Supernatant of the processed samples were stored at −20 °C.

2.8.3. Assessing the in vivo immunogenicity of rhcp entrapped in CS-TPP NPs

2.8.3.1. Total sIgA level in the intestinal lavage and cloacal faecal samples. Presence of rhcp specific total secretory IgA (sIgA) antibody level in the gastric lavage and faecal soup of experimental birds were analysed by indirect ELISA as described previously with minor modifications (Radomska et al., 2016). Briefly, 96 well-ELISA plates were coated with rhcp (1.0 µg/well) diluted in 100 µl of carbonate-bicarbonate buffer (pH 9.6) for overnight at 4 °C. Subsequently, the plates were washed thrice with PBS-T (0.05% Tween 20) and blocked for 1 h at 37 °C with PBS-T containing 5% BSA. Serially diluted lavage

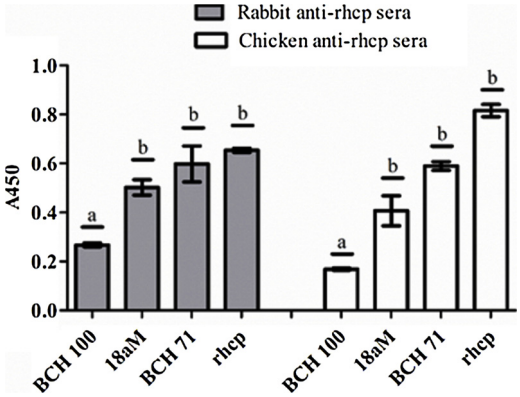

Fig. 4. Specific recognition of native hcp secreted from hcp + *ve* genotype of *C. jejuni* by polyclonal anti-rhcp antibody.
The ability of polyclonal antibody raised against rhcp in recognition of secreted hcp was detected by indirect ELISA method. Culture supernatant collected from two hcp + *ve* genotypes (*18aM and BCH71*) was diluted (2-fold) in carbonate-bicarbonate buffer (pH 9.6) for ELISA while supernatant from hcp-*ve* genotypes of *C. jejuni* (*BCH100*) was used as negative control. *E. coli* expressed rhcp protein was served as positive control. Polyclonal antibody against rhcp raised either in rabbit or chicken were used as the primary antibody (1:1000 dilution). Results indicate specific recognition of native hcp when probed with polyclonal antibody raised either in rabbit (filled bar) or chicken (open bar). No detectable signal was found in the wells coated with supernatant from hcp-*ve* (*BCH100*) culture (Supplementary Fig. S1). Comparative analysis of the ELISA titre confirms no significant difference in terms of immunoreactivity among native and recombinant hcp. Each bar represents the mean absorbance (A450) ± SE of three replicates from two independent experiments. Different letters (a, b) represent statistically significant difference ($P \leq 0.05$).

(2 fold) samples (starting with 1:4 dilution) or faecal soup (started with undiluted sample) were added to each well (100 µl/well) in triplicate and incubated for 2 h at RT. After thorough washing, each plate was incubated with 100 µl of HRP-conjugated Goat anti-chicken IgA (α chain) antibody diluted in 2% blocking buffer (1:2500) for another 1 h at RT. After washing thrice with PBS-T, the plates were developed with 3, 3′, 5, 5′-tetramethylbenzidine, according to the manufacturer's instruction (HiMedia). The reaction was stopped with 50 µl 1 M H_2SO_4 and the absorbance was read at 450 nm using Epoch 2 microplate reader (BioTek, USA). The assay was performed in triplicate and the data represent the Mean ± SE of two independent experiments.

2.8.3.2. Detection of total serum IgY level. Total serum antibody (IgY) levels against rhcp was assessed by indirect ELISA method as described in the previous section. The optimal conditions for the ELISA were determined to be 1.0 µg/well of coating antigen, primary serum dilution of 1:20 (as starting dilution) and 1:2500 dilution of the HRP conjugated Rabbit anti-chicken IgY secondary antibody. The assay was performed in triplicate and the data represent the Mean ± SE of two independent experiments.

2.8.4. Assessment of cytokine gene expression by Semi-quantitative Reverse Transcription PCR (RT-PCR)

Spleen tissues stored in RNA*later*™ were washed thoroughly with PBS and 50 mg of the tissue was homogenized in Trizol reagent and the total RNA was extracted following manufacturer's instruction (Invitrogen, USA). The quantity and quality of RNA for each tissue sample was determined by using Epoch 2 microplate spectrophotometer (BioTek). Approximately 2 µg of RNA was reverse transcribed with MuLV reverse transcriptase using the Superscript Reverse Transcriptase kit following the manufacturer's protocol (BioBharati, India).

To evaluate the cytokine gene expression, primers for chicken IL-1β, IL-8, IL-6, IFN-γ, IL-17 A as well as transcription factor NFkB were obtained from IDT technologies (USA). Details of the primers and amplicon size are mentioned in Table 1. Semi-quantitative PCR for each gene was performed in a volume of 20 µl containing dNTPs, primers, 1X Taq reaction buffer, Taq DNA polymerase, cDNA, nuclease free water. The amount of cDNA used for each gene amplification was normalized on the basis of expression of the house-keeping gene β-actin. Details of the PCR programme was as follow: Initial denaturation at 94 °C for 3 min, followed by 30–40 cycles of amplification at 94 °C for 1 min, 48–58 °C for 1 min., 72 °C for 2 min followed by final extension at 72 °C for 5 min. The data presented here correspond to the mean fold changes calculated with respect to the PBS group using Image Lab™ software (Bio-Rad, USA). The assay was performed in triplicate and the data represent the Mean fold changes ± SE of two independent experiments.

2.8.5. Protective efficacy of intra-gastric delivery of rhcp entrapped in CT-TPP NPs against C. jejuni

At day 7 post last immunization, remaining birds belonging to different groups were orally gavaged with 1×10^8-colony-forming units (CFU) of *C. jejuni*. *C. jejuni* isolate *BCH71* was used as challenge strains in this experiment. *BCH71* was originally isolated from a clinical human sample and genotypic analysis confirmed the presence of major virulence genes (*cad*F$^+$, *hcp*$^+$, *fla*A$^+$, *cdt*B$^+$, *peb*1$^+$, *rac*R$^+$). We chose to use oral gavage challenge as a closer mimic to natural mode of *C. jejuni* entry in chickens.

Seven days after challenge all the birds were sacrificed and one cecum from each bird was collected. The total cecal content was stomached in 5 ml volume of MH broth and serially diluted before plated on Blood Free Campylobacter Selectivity Agar Base media containing CAT supplement. The plates were incubated for 48 h under microaerophilic condition and number of the colonies appeared on the plate were counted. Number of bacterial colonies were expressed as log10 CFU/g for each bird and level of protection was calculated using the following equation:

Log10 units of protection = [mean log10 CFU of the PBS group of birds] – [mean log10 CFU of the other groups]. The assay was performed in triplicate and the data represent the Mean ± SE of three independent experiments.

2.9. Statistical analysis

Origin 8.0 software was used for plotting CD spectra, FT-IR data analysis whereas SEM and TEM data were analyzed for size distribution of the NPs using imageJ software. Data for protective efficacy, Indirect ELISA and semi quantitative RT-PCR were compared between immunized and control (PBS) groups by Student's *t*-test (two tailed, unpaired). $P \leq 0.05$ was considered statistically significant. A GraphPad Prism version 5 software was used to calculate CT_{50} values as well as for the graphics presented in this manuscript.

3. Results

3.1. C. jejuni hcp gene was cloned and expressed in E. coli

Genomic DNA isolated from *C. jejuni* was PCR amplified using hcp specific primers set and an amplicon of 510 bp confirming the size of hcp was purified, restriction digested and cloned into the corresponding enzyme sites of pQE30 plasmid (Fig. 1; Panel A). Sequence analysis confirmed the sequence identity and orientation of hcp gene. Positive transformant recombinant *E. coli* M15 cells harboring pQE30-hcp plasmid were proliferated and induced with IPTG to express rhcp. The SDS-PAGE analysis of the expressed recombinant protein at 20 kDa position confirmed the size and integrity of the purified rhcp while specific detection of immunoblot at similar position confirmed the specificity of the expressed protein (Fig. 1; Panel B).

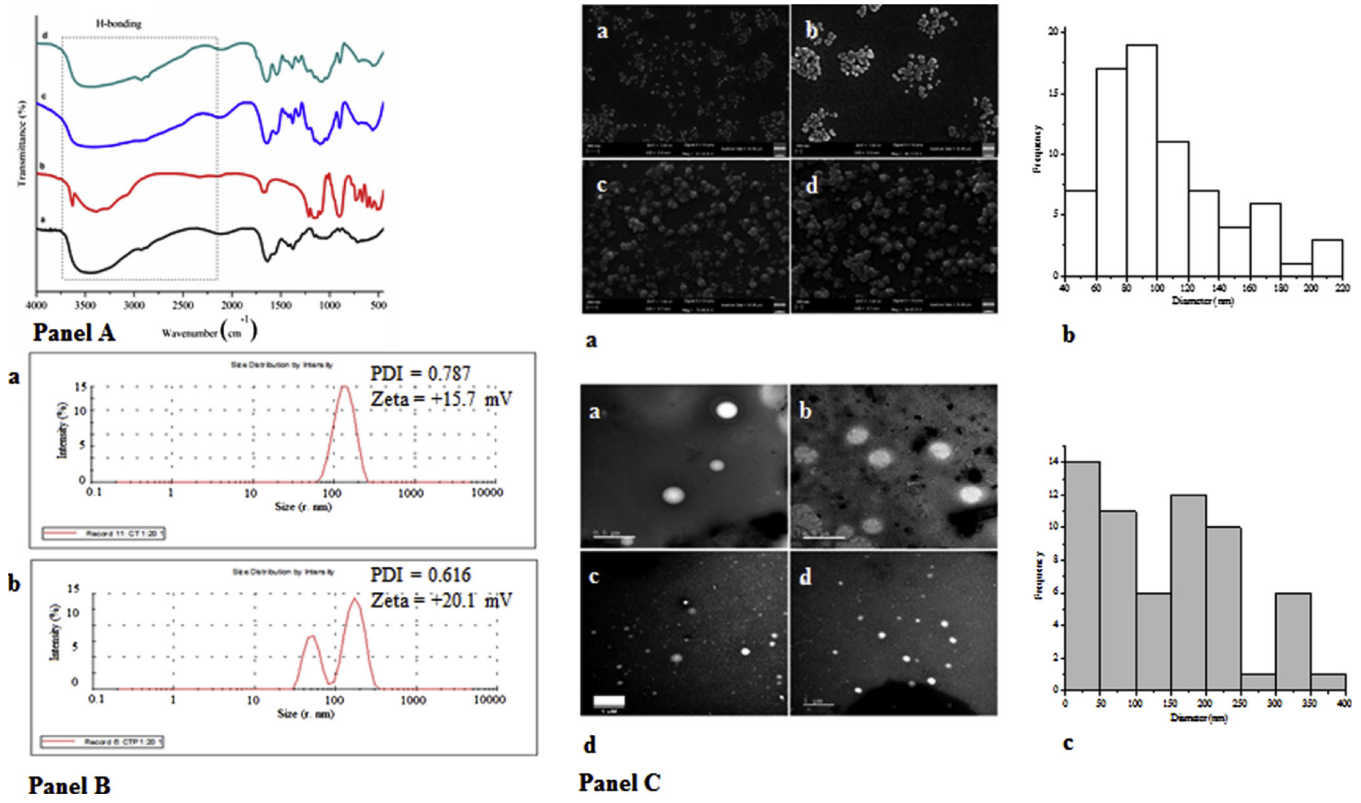

Fig. 5. IR spectrum and hydrodynamic radii distribution of CS-TPP NPs alone or loaded with rhcp and analysis of the morphological features of sham CS-TPP NPs or rhcp loaded NPs by FESEM and TEM.
Panel A: IR spectrum of CS (a), TPP (b), sham CS-TPP NPs (c) and CS-TPP-rhcp NPs (d) were recorded between 4000-500 cm-1. All the spectra were baseline corrected for atmospheric CO_2 and normalized respectively. Presence of spectral band between 2700–3000 cm^{-1} and 1800–1500 cm^{-1} with spectral shift indicates the formation of CS-TPP NPs. Panel B: Hydrodynamic radii distribution of sham CS-TPP (a) and CS-TPP-rhcp (b) nanoparticles suggests even distribution of particle size for sham CS-TPP NPs whereas two different particle distributions were found in case of CS-TPP-rhcp. The distribution of particle diameters is represented by percentage of intensity along with peak radii. Panel C: Scanning electron microphotograph of sham (a, b) or rhcp loaded (c, d) CS-TPP NPs demonstrating island type of aggregation in case of sham CS-TPP NPs with an average size of 97 nm whereas rhcp loaded CS-TPP NPs showing relatively wider distribution of particles size with an average diameter ranged from 34 to 180 nm (a). Statistical analyses of the particle size distribution of sham CS-TPP NPs (open bar) (b) and rhcp loaded CS-TPP NPs (filled bar) (c) are shown. Transmission electron microphotograph of sham (a, b) or rhcp loaded (c, d) CS-TPP NPs showing spherical particles for sham NPs with an average size 60–180 nm while rhcp loaded NPs were found to form comparatively larger particles ranging between 170–300 nm (d).

3.2. Cytotoxicity and $CT_{50}$of purified rhcp was determined

For functional analysis, cell cytotoxicity of rhcp was determined in human and chicken cells by MTT assay. In human INT407, rhcp was found to be toxic with CT_{50} value ˜18.1 μg/ml whereas CT_{50} values for Caco-2 and CEICs were > 30 μg/ml which is in line with earlier study (Bleumink-Pluym et al., 2013) (Fig. 2 and Table 3). The CT_{50} values were further calculated and confirmed by SRB assay (Supplementary Fig. S2).

3.3. Immunoreactivity of rhcp was confirmed

To confirm the immunoreactivity of the purified protein, rabbit polyclonal sera was raised against rhcp and subjected for Western blot analysis. Strong signal intensity of the blot at 20 kDa position confirmed the immunoreactivity of the immunizing antigen (Fig. 3; Panel B). Further the ability of immune sera raised against rhcp in rabbit and chickens to recognize secreted hcp in the culture supernatant of hcp + *ve C. jejuni* was confirmed through indirect ELISA (Fig. 4). Representative well images as well as comparative analysis of the ELISA titre confirm the ability of antibody in recognition of secreted hcp and suggests no significant difference in terms of immunoreactivity when compared to the rhcp (Supplementary Fig. S1).

3.4. Recombinant hcp loaded CS-TPP NPs were synthesized and protein entrapment efficiency was determined

In order to prepare stable NPs, the final concentration of CS to TPP was kept at 0.05%–0.1% (CS:TPP). Because the crosslinking density can influence protein association and release from ionically cross-linked CS-TPP particles, the rhcp was added slowly to the CS solution followed by adding TPP in a drop wise manner into the mixture. A total 70 μg of protein was used initially however approximately 50 μg was found to finally incorporated in NPs, thus the entrapment efficiency of the particles was calculated to be 70% of the initial protein amount.

3.5. Physical property and morphology of CS-TPP NPs

3.5.1. FT-IR

FT-IR spectra of different component of the NPs alone or in a cross-linked state is presented in (Fig. 5; Panel A). Pure chitosan (CS; a-black line) was shown to have broad band at 3460 cm^{-1} possibly due to the OH stretching. The bands at 2948, 2867, 1437, 1367 and 1169 cm^{-1} positions are assigned to the CH_2 bending due to pyranose ring (Pawlak and Mucha, 2003). In case of CS-TPP NPs (c-blue line), the peak of 3460 cm^{-1} shifted to 3290 cm^{-1} and became wider with increased relative intensity indicating an enhancement of the hydrogen bonding. The major differences noted between the spectra of the CS-TPP NPs and free CS, refers to the weak bands at 1218 cm^{-1} which could be assigned

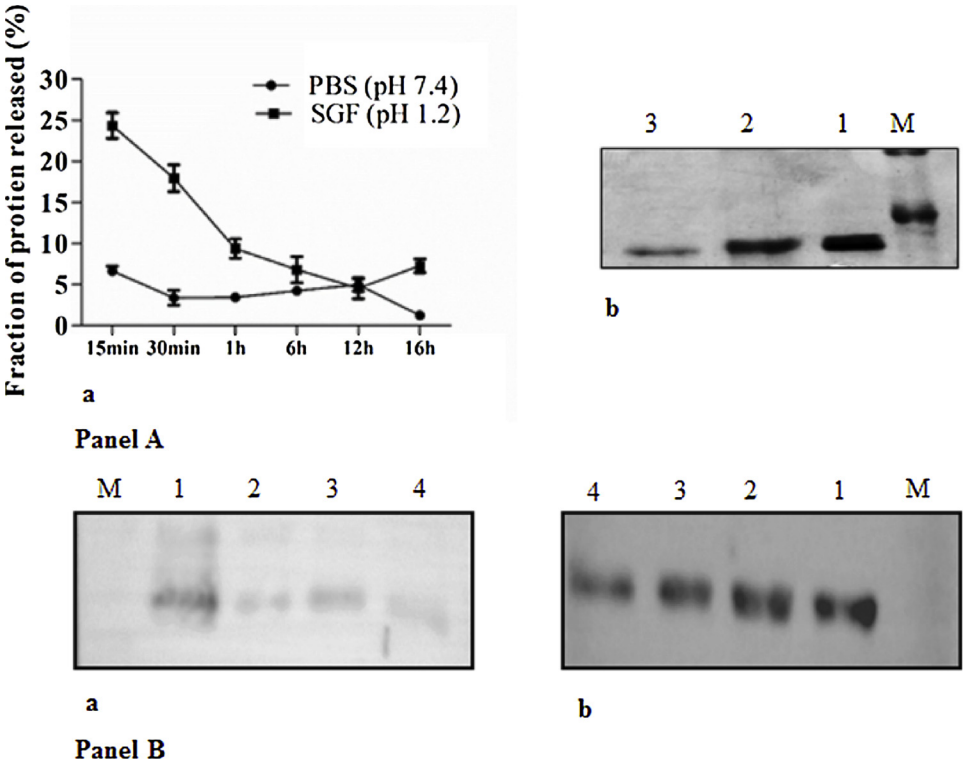

Fig. 6. *In vitro* release kinetics of rhcp from CS-TPP NPs, protein integrity and Western blot analysis.
Panel A: *In vitro* release kinetics of entrapped rhcp was assessed in phosphate buffered saline (PBS; pH 7.4) and simulated gastric fluid (SGF; pH 1.2). Lines indicate controlled, linear and slower release of rhcp when NPs were incubated in PBS while rapid release of rhcp was noticed at first 30 min before reaching a plateau (a). SDS-PAGE profile of rhcp from destabilized NPs after 16 h of incubation either with PBS or SGF suggest the integrity of the entrapped protein (b). Lane: M: Marker; 1: purified rhcp; 2: rhcp in SGF; 3: rhcp in PBS. Panel B: Western blot analysis of released rhcp in SGF using rabbit polyclonal anti-rhcp antibody (a) as well as mouse monoclonal anti-His antibody (b). Immunoblot at expected size indicate that the immunoreactivity of the released protein remains unaltered. Lane: M: Marker; 1: rhcp, 2-4: released rhcp in SGF.

to P—O stretching signal and band at 905 cm^{-1} attributed to P—O—P asymmetric stretching. Additionally, the observed peak at 1670 cm^{-1} along with the previously described signals indicate the presence of phosphate groups in the CS-TPP NPs (Luo et al., 2010; Vasconcellos et al., 2011). The band at 1088 cm^{-1}, assignable to the stretching of C–O bonds of primary alcohols changes its position noticeably in NPs (c-blue line; d-green line). Such changes were attributed to interaction between CS and TPP (b-red line) (Vasconcellos et al., 2011). The band at 1646 cm^{-1} that appeared on CS spectra, attributed to N—H deformation of amine groups, was merged with TPP signal at 1670 cm^{-1} and produced a new sharp peak at 1542 cm^{-1} in CS-TPP or CS-TPP-rhcp particles, this could be assigned to NH_3^+ bond formation with TPP (Luo et al., 2010; Vasconcellos et al., 2011). Based on the decoded FT-IR information, crosslinking through ionic interactions among negatively charged phosphate groups of TPP and protonated NH_3^+ units of CS chain could be concluded. The minute differences and broadness of spectra ranging from range from 3646 to 2518 cm^{-1} in NPs in comparison to free CS or TPP might be due to the extended and diversified H-bonds networks among CS-TPP chains. The subtle nature of the FT-IR spectra further explained as the pronounced interaction between amino and hydroxyl group on CS chains.

3.5.2. Morphology, size distribution and surface charge of NPs

Data obtained from DLS showed single peak suggesting relatively uniform size distribution for CS-TPP NPs. The average hydrodynamic radii were noted as 257 nm (PDI = 0.787) and 167 nm (PDI = 0.616) for CS-TPP and CS-TPP-rhcp NPs respectively. In comparison to free CS-TPP NPs, two peaks were obtained in case of CS-TPP loaded with rhcp (Fig. 5a and b; Panel B). In terms of net surface charge, zeta potential (ζ) of the NPs suggests overall positive charge for both forms of NPs. For CS-TPP NPs it was found to be + 15.7 mV while loading with rhcp was found to increase the surface charge to + 20.1 mV. This may be attributed to conjugation of rhcp to CS-TPP NPs. Considering the overall surface charge of the protein which would be positive at pH 5.4 where the NPs were synthesised, additional surface charge of CS-TPP NPs thus attributed to rhcp loading (Sims, 2010).

Analysis of CS-TPP NPs using FESEM suggest the spherical morphology of the NPs with comparatively narrow particle size distribution when compared with rhcp loaded NPs (Fig. 5a; Panel C). The average size distribution of CS-TPP NPs were analysed to be 97 ± 5.0 nm (Fig. 5b; Panel C; Open bar) whereas rhcp loaded CS-TPP NPs were found to have higher radii with wide particle diameter distributions. Based on the analysis of the average particle size rhcp loaded CS-TPP NPs were found to be ranged from 180 ± 6 nm to 34 ± 7 nm (Fig. 5c; Panel C; Filled bar).

Morphology and particle size of both type of NPs were further analysed using TEM. Spherical NPs were observed which is in correlation with SEM data. Average particle size analysed for CS-TPP NPs ranging from 60 to 180 nm and for CS-TPP-rhcp it was 170–300 nm in size (Fig. 5d; Panel C).

3.6. In vitro release of rhcp from CS-TPP NPs was determined

Protein release profile from CS-TPP NPs in PBS (pH 7.4) and SGF (pH 1.2) is shown in (Fig. 6a; Panel A). The fractions of rhcp released from CS-TPP NPs in the suspending solution suggest that the protein release is maximum within the first 15–30 min (24% and 18%) in case of SGF while an opposite characteristic was found for CS-TPP NPs when incubated in PBS (6% and 3%). However, the protein release was found to be sustained and controlled in subsequent time points in both buffer without notable difference.

3.7. Protein integrity of entrapped rhcp into CS-TPP NPs was analyzed

3.7.1. Protein integrity of entrapped and released rhcp was confirmed

To confirm the integrity of rhcp entrapped in CS-TPP NPs, NPs recovered from the Section 3.6 was destabilized with 10% NaCl. Presence of protein band corresponding to the size of rhcp confirmed the protein integrity in both PBS and SGF (Fig. 6b; Panel A). The phenomenon of more protein release in SGF can be attributed due to the increased destabilization in the mentioned fluid. SGF itself destabilized and loosen up the entrapped protein in CS-TPP-rhcp NPs where after addition of 10% NaCl further destabilize the protein layer which finally increase the released protein content as evident from gel image. On the

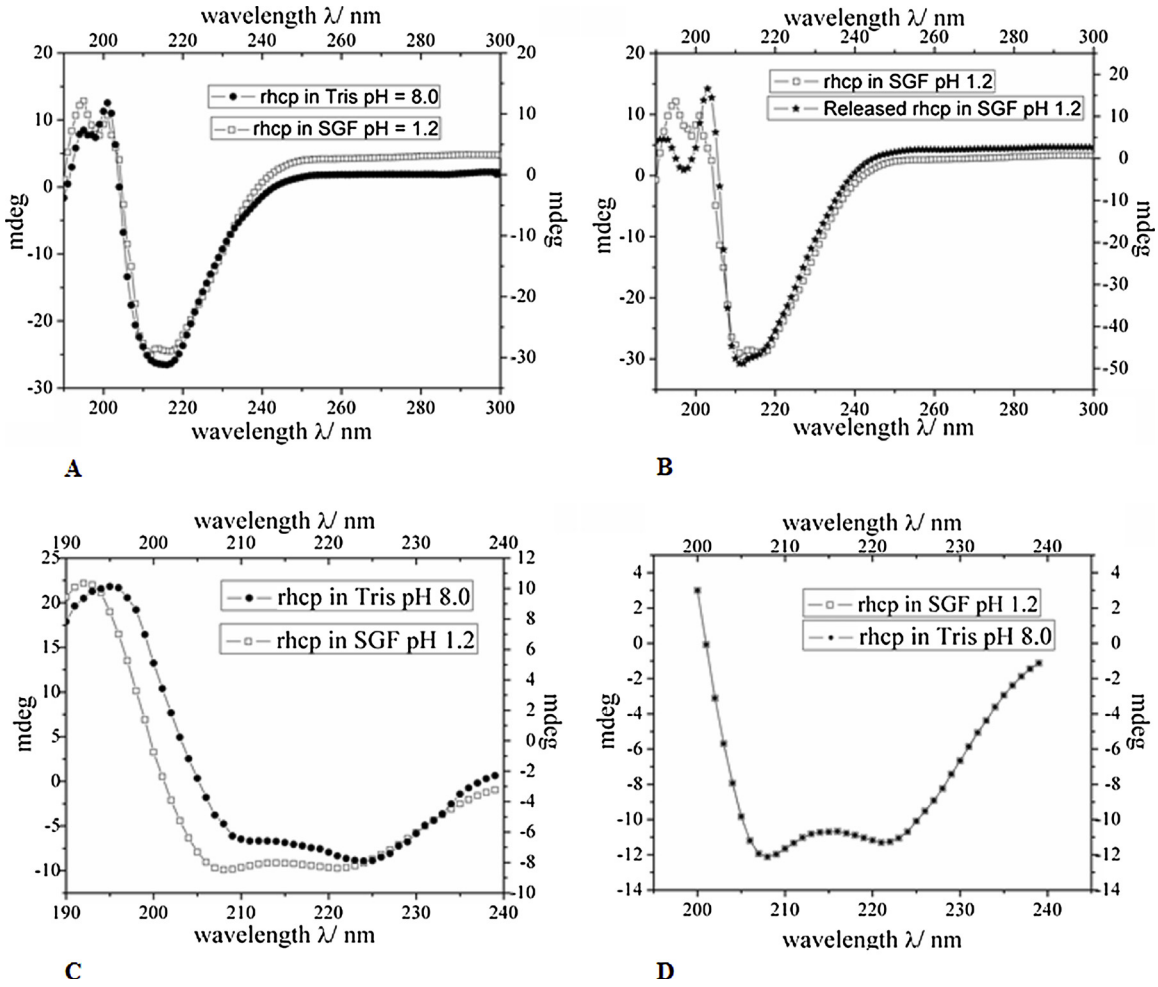

Fig. 7. Far-UV CD spectroscopic analysis of rhcp as a function of pH (8.0 and 1.2).
(A) Experimental CD spectrum of rhcp in Tris buffer pH 8.0 (filled dots) and SGF pH 1.2 (open square) at 25 °C. (B) Experimental CD spectrum of released rhcp in SGF (filled star) and rhcp in SGF (open square) at 25 °C. Average data plot has been done from three repeated data acquisition in the instrument. (C) Theoretical fitting/prediction of experimental data for possible helical structures (α-helix and β-sheets) using K2D2 online server for the data range of 190–240 nm and (D) for data range of 200–240 nm.

other hand, PBS did not impose such additional destabilizing factor as observed in SGF. Further, western blot analysis of released rhcp when probed either with monoclonal or polyclonal antibodies confirmed the specific recognition of epitope/s present in rhcp (Fig. 6a and b; Panel B).

3.7.2. Structural conformation of released rhcp was confirmed

To study the changes in structural conformation of rhcp, protein's secondary structure when analysed through CD at two different pH (pH 8.0 and 1.2), no significant difference in the conformation with respect to α-helix or the β-sheets was observed. However, a minor noise as observed in the far-UV region (190–200 nm) of CD spectrum of rhcp in SGF, a 5-point smoothing was performed to represent the spectral overlap using second order polynomial fitting (Fig. 7A). Whether the observed difference have any effect on protein structure, the distribution of α-helices and β-strands at two different pH were predicted using online based server K2D2 (Fig. 7C and D; Table 4).

Correspondingly, CD spectra of released rhcp when probed in SGF (pH 1.2), except some minor differences in the dip region of spectra, two distinct peaks were observed at 211 nm and 216 nm in both the cases. In contrast, when CD spectra of peak region were compared, a minor shift and change in intensity ratio were noticed (released rhcp: 202 nm and 192 nm Vs rhcp: 201 nm and 195 nm) (Fig. 7B).

3.7.3. Cell cytotoxicity of released rhcp was determined

To confirm the cell cytotoxicity of CS-TPP NPs and released rhcp MTT assay was performed. For sham CS-TPP NPs, CT_{50} value was > 30 μg/ml in INT407. The CT_{50} values for released rhcp was determined to be 21.1 μg/ml for INT407 and > 30 μg/ml for Caco-2 and CEICs (Fig. 8 and Table 3). The CT_{50} values were further confirmed by SRB assay (Supplementary Fig. S2).

3.8. Intra-gastric delivery of rhcp loaded CS-TPP NPs positively affect hcp specific local and systemic immune response in chickens

Indirect ELISA assay using intestinal lavage collected from birds belonging to different experimental groups suggests significant rise in sIgA level in birds orally gavaged with CS-TPP-rhcp and IFA-rhcp immunized group when compared with the birds received only sham NPs or PBS ($P \leq 0.05$) (Fig. 9; Panel B).

To monitor the mucosal and systemic antibody response in immunized birds, cloacal faeces and sera samples collected at different time points post immunization were evaluated. A steady and consistently higher increment of sIgA level in cloacal faeces was recorded in CS-TPP-rhcp group followed by IFA-rhcp immunized group throughout the experiment period and reached to maxima at day 21 post first immunization (Immunized Vs Control group; $P \leq 0.05$) (Fig. 9; Panel C). In addition, high level induction of serum antibody

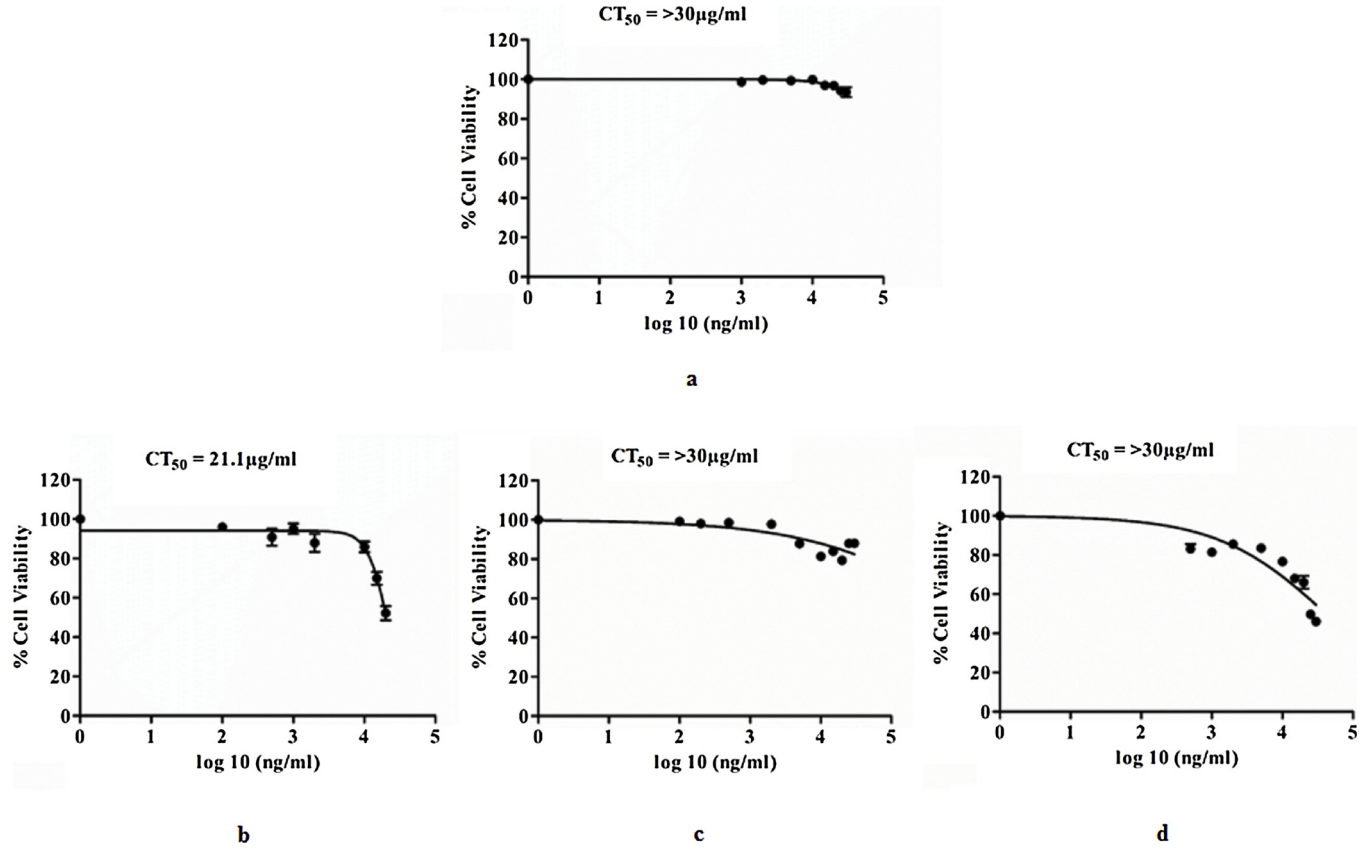

Fig. 8. Cytotoxicity of CS-TPP NPs and released rhcp in human INT407, Caco-2 and CEICs.
Cytotoxicity of CS-TPP NPs in INT407 by MTT assay using different concentration of NPs (0.1 µg/ml to 30 µg/ml) suggest that NPs used in this study is non-toxic within the range of NPs concentration used in this study (a). The functional analysis (cell cytotoxicity) of released rhcp was assessed in human INT407 (b), Caco-2 (c) and CEICs (d) by MTT assay. The CT_{50} of the released rhcp for INT407 cells was calculated as 21.1 µg/ml while in case of Caco-2 or CEICs, it was found to be > 30 µg/ml. Each data point represent the mean cell viability ± SE relative to untreated cells normalized to 100% of two independent experiments.

(IgY) was also observed in birds administrated with rhcp either orally or systemically (Immunized Vs Control group; $P \leq 0.05$) (Fig. 9; Panel D). It is also noteworthy to mention that birds received sham NPs showed higher background in case of ELISA assay using faecal pellet.

3.9. Transcriptional upregulation of Th1 and Th17 type cytokines

Transcriptional analysis of cytokine genes expressed in spleen tissue were analysed by semi-quantitative RT-PCR and fold change was calculated with respect to PBS control group (Fig. 10). Fold change of cytokine gene suggests marked up-regulation of NFkB, IL-1β, IL-8, IL-6, IFN-γ in birds orally gavaged with CS-TPP-rhcp compared to PBS control (CS-TPP-rhcp Vs PBS control; $P \leq 0.05$). However, when compared with the PBS control, immunization with IFA-rhcp was found to be comparable with CS-TPP-rhcp in terms of IL-6 and IFN-γ gene expression (IFA-rhcp Vs PBS Control; $P \leq 0.05$).

In terms of IL-17 A gene expression, significant expression was noticed in CS-TPP-rhcp and IFA-rhcp immunized group followed by sham CS-TPP NPs group in comparison with PBS control group (Immunized Vs PBS Control; $P \leq 0.05$).

3.10. Intra-gastric administration of CS-TPP entrapped rhcp significantly reduceC. jejunicolonization in cecum

To assess the efficacy of mucosal delivery of rhcp loaded CS-TPP in the reduction of *C. jejuni* colonization in the ceca, the bacterial burden was calculated at day 7 post challenge with *C. jejuni*. Data presented in (Fig. 11) indicates significant reduction in the number of bacterial load in birds orally administered with CS-TPP-rhcp (˜1.0 log unit) when compared to either IFA-rhcp (˜0.5 log unit) immunized birds or unimmunized control groups of birds ($P \leq 0.05$).

4. Discussion

Campylobacter contaminated poultry and poultry products are the major sources for foodborne gastroenteritis in human (Rosenquist et al., 2006). A number of case-studies have strikingly reported the significant correlation between human infection with *C. jejuni* and the consumption of contaminated raw or undercooked poultry (Allos, 2001; Hermans et al., 2011; Skarp et al., 2016; Suzuki and Yamamoto, 2009). *C. jejuni* uses several strategies to survive and persistently colonize in chickens gut with little or no host pathology (Beery et al., 1988; Conlan et al., 2007; Hendrixson and DiRita, 2004; Smith et al., 2008). With the accumulating evidences that suggest the emergence of new drug resistance *C. jejuni* strains, the risks of human infection have substantially increased (Bae et al., 2014; Brown et al., 2015). Considering the uprising global awareness against the injudicious use of antibiotic in food animals, therapeutic use of antimicrobial in poultry is very restricted. Therefore, developing effective prophylactic strategy remains the most promising approach to combat *C. jejuni* infection in chickens.

Among the various vaccination strategies against *C. jejuni* in poultry, oral vaccination with whole-killed *C. jejuni*, recombinant protein-based vaccines are of note. With the recent advances in our understanding of *C. jejuni* colonization of chickens, several surface exposed colonization protein (SECPs) of *C. jejuni* that promote bacteria adherence and cell invasion, have emerged as potential vaccine candidate with variable success (Kobierecka et al., 2016a, b; Neal-McKinney et al., 2014; Theoret et al., 2012). Considering the role of mucosal immune system

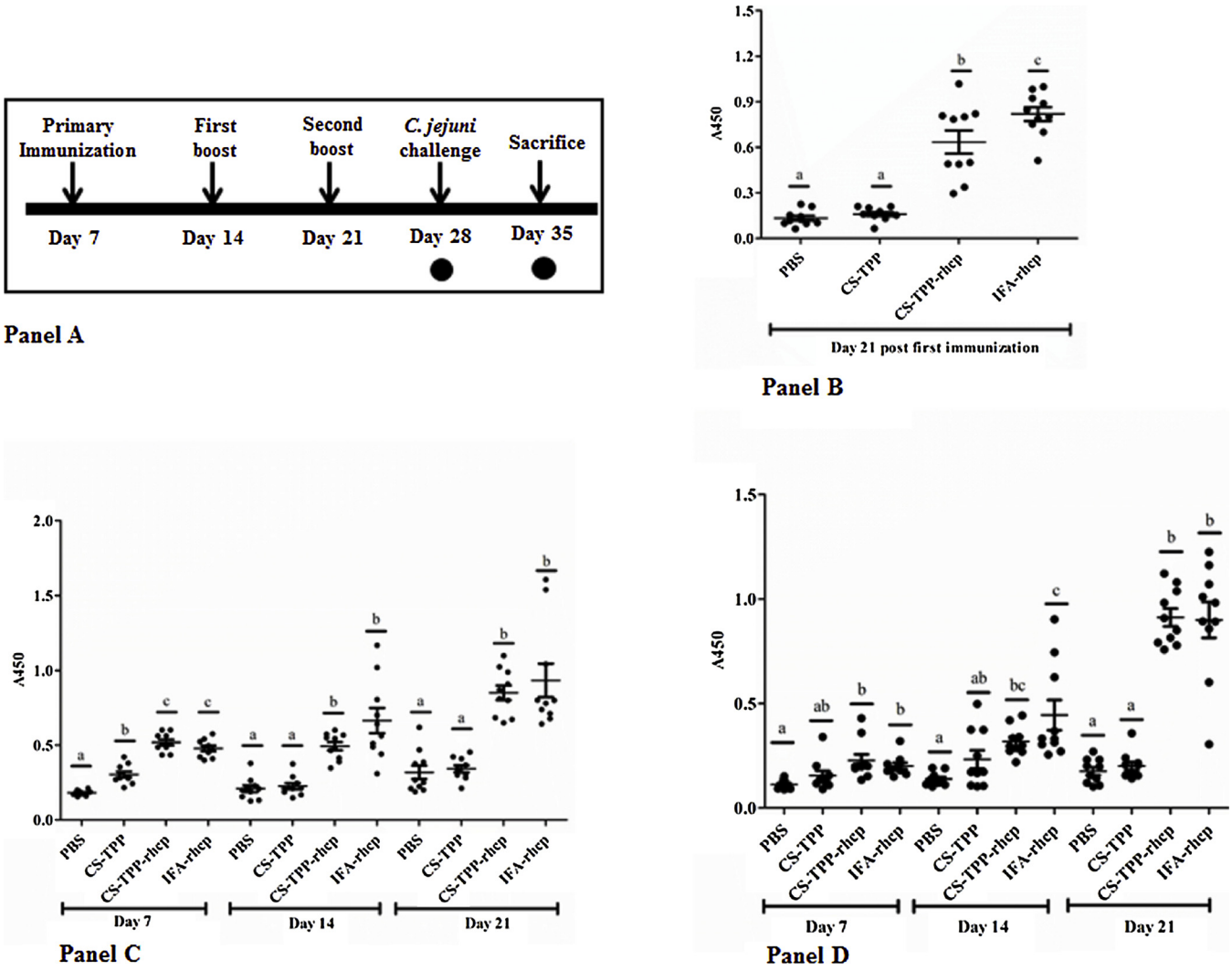

Fig. 9. Schematic representation of the chicken immunization schedule and comparative analysis of rhcp specific mucosal (sIgA) and systemic immune (IgY) responses in chickens.

The experimental birds were immunized at the indicated time-intervals by either intra-gastric administration (gavage) of rhcp loaded NPs or sham NPs or subcutaneous injection (s/c) of rhcp-emulsified in IFA. Birds orally gavaged with sham NPs or PBS were kept as control. Black circles indicate the day of sacrifice (Panel A). Levels of intestinal (sIgA) and serum (IgY) antibodies against rhcp antigens were determined by indirect ELISA. Anti-rhcp sIgA levels were measured in the intestinal lavage (Panel B) and cloacal faeces (Panel C) while total IgY level was measured in the sera sample (Panel D) collected at different days post first immunization time points. Purified rhcp protein was used as coating antigen (1 μg/well). Individual dot represents the antibody titre in intestinal lavage sample (1:16 dilution), cloacal faeces (1:64 dilution) and sera sample (1:80 dilution). Data represent the mean antibody titre (A450) ± SE of 10 birds/group from two independent experiments. Mean antibody titre of immunized groups was compared to unimmunized control group (received PBS only). Different letters (a, b, c) represent statistically significant difference among groups ($P \leq 0.05$).

in conferring host defence against *C. jejuni*, the use of live vectored or nanoparticle based oral delivery of several *C. jejuni* proteins namely as Cja A, Cja D, Dps, as well as outer-membrane proteins (OMPs) were also reported in the past (Annamalai et al., 2013; Buckley et al., 2010; Clark et al., 2012; Laniewski et al., 2014; Layton et al., 2011; Rice et al., 1997; Theoret et al., 2012; Wyszynska et al., 2004).

In recent times, with the emergence of T6SS in *C. jejuni*, genes encoding effector proteins of T6SS cluster have attracted significant attention for their distinct functions and expressive contribution in enhancements bacterial virulence and cell cytopathies (Bleumink-Pluym et al., 2013; Lertpiriyapong et al., 2012; Pukatzki et al., 2009; Silverman et al., 2012). Although, the exact role *C. jejuni* T6SS in influencing campylobacteriosis in human is yet to be established, a growing body of data including our recent study suggest that T6SS mediated pathogenesis is mostly attributed to hcp protein (Bleumink-Pluym et al., 2013; Harrison et al., 2014; Kuskonmaz et al., 2009; Lertpiriyapong et al., 2012; Noreen et al., 2018; Sainato et al., 2018). The role of hcp in enhancement of bacterial motility, biofilm formation as well as bacterial invasion and host cell adherence has been proposed in the recent past while several other studies have examined the value of hcp immunization in conferring protection against different Gram negative bacteria (Burtnick et al., 2011; Suarez et al., 2010, 2008; Wang et al., 2015; Whitlock et al., 2010; Yang et al., 2017). However, the potential of hcp protein as a prospective vaccine candidate in the light of blocking *C. jejuni* colonization in chickens has never been explored in the past.

In line with our central hypothesis of reducing the degree of *C. jejuni* inhabitancy in the chickens intestine will reduce the risk of human infection, the present study explored the benefit of hcp immunization against *C. jejuni* in chickens. Considering that gut mucosa offers the apposite site for *C. jejuni* adherence (Alemka et al., 2012) and invasive mode of immunization in food animal such as chickens have several implications, it was of our interest to establish a safe and efficacious mucosal vaccine composition to offer effective immune-protection

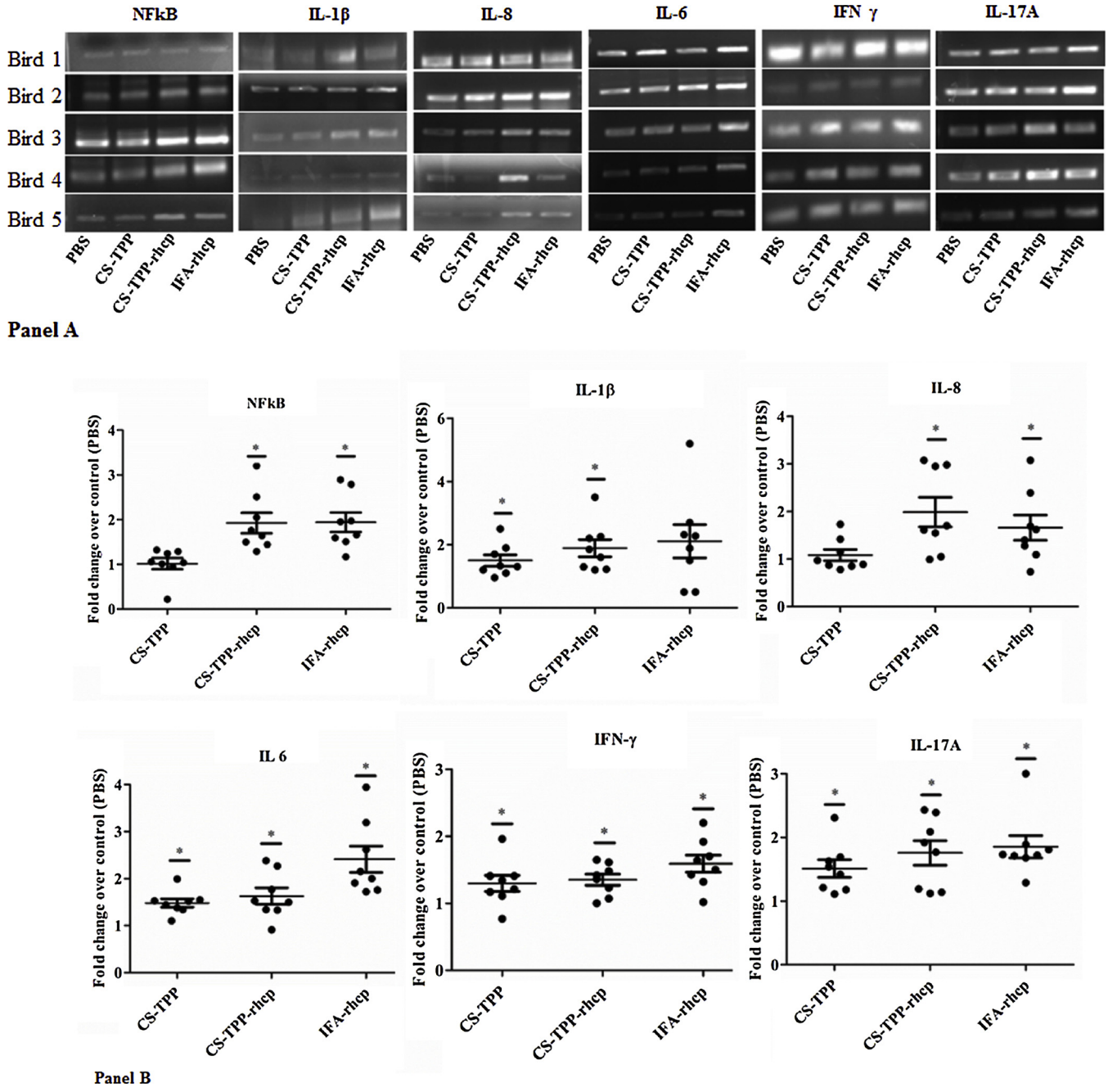

Fig. 10. Comparative analysis of cytokine gene expression in spleen.
Spleen tissues collected from experimental chickens (n = 8) on day 7 post last immunization were processed for RNA extraction followed by synthesis of cDNA for cytokine gene expression study. Panel A: Representative gel images of semi-quantitative RT-PCR showing mRNA expression of transcription factor NFkB and cytokines (IL-1β, IL-8, IL-6, IFN-γ and IL-17 A). Panel B: Fold changes of cytokine gene expression in response to sham CT-TPP, CS-TPP-rhcp and IFA-rhcp immunization. Fold changes was calculated with respect to unimmunized control group (received PBS only). Data represent mean ± SE of 8 birds/group from two independent experiments. Symbol * represents statistically significant difference with respect to the birds received PBS only ($P \leq 0.05$).

against *C. jejuni*. Owing to the several advantages exhibited by chitosan including safety, biocompatibility, biodegradability, low immunogenicity and mucoadhesive properties, we chose to use chitosan-based NPs as a candidate for hcp protein delivery to chicken's gut mucosal surface (Agnihotri et al., 2004; Pandey et al., 2005; Plapied et al., 2010; Sayin et al., 2009).

The sequential assessment of sera, intestinal lavages fluid and cloacal faeces revealed that the prime-boost immunizations of rhcp either orally or systemically can significantly augment hcp specific local (sIgA) or systemic (IgY) antibody responses. It is of note that antigen-presenting cells including naïve B cell in gut associated lymphoid tissue (GALT), upon exposure to antigen, travel to the mesenteric lymph node (MLN) where they undergo clonal expansion and release into the systemic circulation (Macpherson and Smith, 2006). Given that the hcp protein primarily expressed in the bacterial outer membrane, marked sIgA antibody response in the intestine suggest the accessibility of B cell epitopes present in the exposed domain of hcp when delivered via CS-TPP NPs. The details of B cell specific epitopes predicted by using database IEDB is presented in Table 2.

As numerous naturally N-linked glycosylated proteins including proteins within T6SS (formerly T4SS) cluster (VirB10) of *C. jejuni* were shown to influence the antigenicity as well as host immune responses,

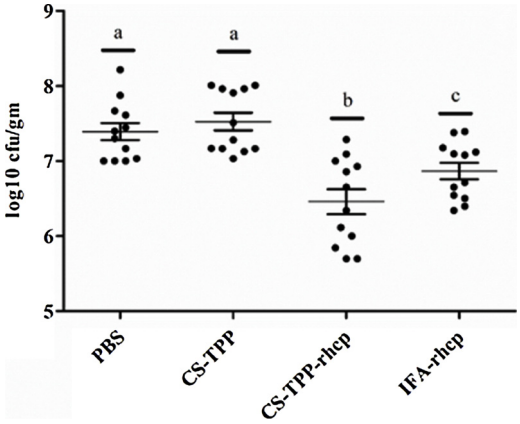

Fig. 11. Effect of rhcp immunization in *C. jejuni* colonization in ceca.
Birds received three doses of rhcp either orally or subcutaneously were challenged with 1×10^8 CFU of *C. jejuni* orally at day 7 post last immunization. Control birds were given either PBS or sham NPs (infected but not immunized). Seven days after the challenge all the birds were sacrificed and viable *C. jejuni* were recovered from the necropsied ceca. Significantly lower number of bacterial recoveries was noted in CS-TPP-rhcp immunized group as compared to either IFA-rhcp group or unimmunized birds ($P \leq 0.05$). Data represent mean ± SE of 12 birds/group from three independent experiments. Different letters (a, b, c) represent statistically significant difference among groups ($P \leq 0.05$).

Table 2
List of predicted linear B cell epitopes and N-glycosylation site in *C. jejuni* hcp protein.

*S. No.	Start	End	Peptide	Length
1	14	36	QGLISSGASTEASIGNRYKSGHE	23
2	48	66	VTVPVDQQSGQPSGQRVHK	19
3	101	108	TSTSGGSE	8
4	125	138	LIMPNAQESSNHDK	14
5	156	169	TAAGTSGSDDWREG	14

#MAEPAFIKIEGSTQGLISSGASTEASIGNRYKSGHEDEIMAQEVSHIVTVPVDQQSGQPSGQRVHKPFSFTCSLNKSVPLLYNALTKGERLPTVEVHWFRTSTSGGSEHFFTTKLEDAIITNIELIMPNAQESSNHDKTELLKVSMSYRKVVWEHTAAGTSGSDDWREGK.

#NetNGlyc 1.0 Server was used for the prediction of potential N-glycosylation site (1.0 at 75th position) in the sequence of *C. jejuni* hcp. Consensus sequence for N- glycosylation acceptor site (Asn-X-Ser/Thr) is underlined.

* Data base IEDB was used for epitope prediction.

Table 3
Cytotoxicity of purified rhcp and released rhcp protein.

Proteins	CT_{50} values (μg/ml)					
	INT407		Caco-2		CEICs	
	MTT	SRB	MTT	SRB	MTT	SRB
rhcp	18.1	17.4	> 30	> 30	> 30	> 30
Released rhcp	21.1	22.5	> 30	> 30	> 30	> 30

Table 4
Distribution of α-helices and β-sheet of rhcp in Tris (pH 8.0) and SGF (pH 1.2).

rhcp	190-240 nm		200-240 nm	
	α-helices	β-sheet	α-helices	β-sheet
Tris buffer, pH 8.0	56.26%	5.69%	84.27%	1.24%
SGF, pH 1.2	67.22%	2.22%	84.27%	1.24%

we further looked for N-glycosylation acceptor sequence within hcp sequence (Alemka et al., 2013; Karlyshev et al., 2004; Larsen et al., 2004; Pei et al., 1998; Szymanski et al., 2002). In the available crystal structure of native form of hexameric hcp of *C. jejuni* (PDB code 6A2V) (Noreen et al., 2018) the predicted consensus sequence (Asn-X-Ser/Thr) for N-glycosylation was found to be buried at the interface of the two monomer of hcp subunits without interfering B cell epitope. This arrangement makes the Asparagine inaccessible for N-glycosylation in the complete hexameric form (Table 2 and Supplementary Fig. S3). Since glycosylation in *C. jejuni* occurs post-translationally, with respect to inaccessible consensus sequences, the possibility of N-linked glycosylation on the structural stability of the hexameric complex of hcp needs to be investigated.

The supposition was further confirmed by demonstrating specific recognition of both native as well as recombinant form of protein (non-glycosylated) using anti-rhcp antibody (Fig. 4). Additionally, chicken sera from the strongly reactive experimental group that were immunized with either CS-TPP-rhcp or IFA-rhcp showed specific immunoblot at the expected size of hcp further suggest the specific reactivity of the immunized sera against rhcp protein (blot not shown). Previously, also modification or complete elimination of N-glycosylation of several other *C. jejuni* proteins, including ZnuA or JlpA, Cj0263 and Cj1496c were found to be inconsequence in terms of protein functionality or their overall antigenicity (Davis et al., 2009; Kakuda and DiRita, 2006; Kakuda et al., 2012; Scott et al., 2009). Together with our prediction, the data obtained from cell cytotoxicity and indirect ELISA allow us to conclude that N-glycosylation of hcp may have little effect on the overall antigenicity of rhcp protein expressed in *E. coli* host.

Though mucosal administration of recombinant protein is as not as easy as systemic immunization, CS-TPP NPs seem to offer effective antigen presentation with improved safety of immunogen during gut transit (Arca et al., 2009). It is worth noting that nano-sized particulate carriers often possess increased antigen contact area and thereby facilitate better antigen presentation than bigger sized micro or macroparticles (Yan et al., 2013). With larger surface area, higher dispersibility, unique mucoadhesive property related to high positive charge density of CS-NPs, in the present study the predicted utility of CS-TPP NPs was achieved.

Moreover, together with higher level of biosafety, increased thermal and solution stability of CS NPs as shown by us, could be the additional benefits of CS based NPs towards developing novel immunization approach particularly against warm blooded vertebrates such as avian (Kamat et al., 2015; Malmo et al., 2011). In view of the immune response generated against the larger carrier molecules or delivery vehicle often limit the use of antigen carrier, here we also claim the use of chitosan based non-protein NPs would be safe, non-immunogenic antigen carrier system with little or no anti-system response in chickens.

As *C. jejuni* is an intracellular pathogen, it was of our interest to see if the observed humoral immune response afforded by the mucosal administration of rhcp modulate the cellular immune response. Therefore, next we investigated the effect of intra-gastric administration of rhcp in T cell activation in immunized birds. We observed that the local and systemic antibody response afforded by hcp associated cellular responses with a mixed Th1 and Th17 profile as evident from marked upregulation of NFkB, IFN-γ, IL-1β, IL-8, IL-6 and IL-17 A genes expression. The enhanced ability of hcp^+ *C. jejuni* genotypes in bacterial adherence and invasion to human and chickens cells as shown by us and others suggest the possible role of hcp in bacterial T6SS mediated virulence (Corcionivoschi et al., 2015; Singh and Mallick, 2019). However, the direct role of hcp in the evasion of host immune response was explicitly studied in *Aeromonas hydrophila* mutant model by demonstrating that supplementation of hcp could significantly inhibit the expression of major pro-inflammatory cytokines to promote IL-10 and TGF-β expression (Suarez et al., 2010). Taken together, with the ability of hcp immunization in triggering the release of a set of cytokines that

initiate Th1-type immune responses in chickens may have contributed in the host protection as observed in this study.

Nevertheless, the intrinsic mechanisms by which hcp regulate the skewing of Th17 polarization need to be elucidated in more detail. However, the Frequentist and Bayesian structural equation models (SEM) based on the combinations of experimental and statistical modelling, suggest Th17 upregulation in response to *C. jejuni* infection could offer host protection in broiler chickens (Reid et al., 2016). To this end, the marked expression of IL-1β and IL-6 genes with significant upregulation of IL-17 A as observed in the present study corroborates the value of hcp immunization in Th17 cell differentiation (Chung et al., 2009). Given that the expression of IL-1β and IL-6 is known to have a strong correlation with IL-17 A production, activation of mixed Th1 and Th17 type of response by mucosal delivery of hcp appears to be positively contributed in host protection against *C. jejuni* challenge (Smith et al., 2008).

Finally, to test the value of mucosal immunization in blocking of bacterial colonization, immunized birds were challenged with *C. jejuni* harbouring functional T6SS. Significant reduction in cecal load of *C. jejuni* compared to the control birds indicates the benefit of mucosal delivery of rhcp. Although immunization of rhcp with IFA resulted in robust systemic (IgY) and mucosal (sIgA) antibody response, when compared to the mucosally administered group, systemic immunization was found to be less effective in terms of reduction in cecal load of *C. jejuni*. Hence, present study acclaims the importance of anti-hcp immune response generated in the mucosal surface in blocking gut colonization of *C. jejuni* in chickens. Since hcp gene possess higher sequence conservation amongst the other *C. jejuni* strains as well as other T6SS bearing gut pathogens, although not tested in this study, the immune response induced by hcp immunization is predicted to be protective against a wide range of *C. jejuni* including other mucosally important gut pathogens.

5. Conclusions

Taken together, we suggest that hcp could serve as effective vaccine candidate against *C. jejuni* in chickens as well as in other susceptible hosts. Given that systemic immunization would be time consuming, labour-intensive and costly, mucosal immunization of hcp could serve as a promising alternative when large numbers of flocks are needed to be immunized against *C. jejuni*.

Ethics statement

The rabbit and chicken experimentation protocol were approved by Institute Animal Ethics Committee (IAEC), Indian Institute of Science Education and Research Kolkata and all procedures were conducted in accordance with the Committee for the Purpose of Control and Supervision of Experiments on Animals (CPCSEA) guidelines, MoEF & CC, Govt. of India. Permit number of the experimental protocols approved by the IAEC was IISERK/IAEC/OA/2018/001.

Author contributions

AIM and AS designed the experiment, performed the experiment, analysed the data and wrote the manuscript. KN contributed in cloning and expression of rhcp used in this study. SB helped in physical characterization of CS-TPP nanoparticles, CD study and data interpretation.

Conflicts of interest

The authors declare that no conflict of interest regarding the publication of this article.

Acknowledgments

This work was supported by a grant from Department of Biotechnology, Govt. of India (Grant No. BT/PR21437/ADV/90/248/2016). The authors thankfully acknowledge Dr. Rahul Das, Assistant Professor, Dept. of Biological Sciences, IISER Kolkata for his input in structural analysis and Dr. Asish K. Mukhopadhaya, Principal Scientist, NICED, Kolkata for providing human clinical isolates of *C. jejuni*.

Appendix A. Supplementary data

Supplementary material related to this article can be found, in the online version, at doi:https://doi.org/10.1016/j.molimm.2019.04.016.

References

Abkar, M., Fasihi-Ramandi, M., Kooshki, H., Sahebghadam Lotfi, A., 2017. Oral immunization of mice with Omp31-loaded N-trimethyl chitosan nanoparticles induces high protection against Brucella melitensis infection. Int. J. Nanomed. 12, 8769–8778.

Agnihotri, S.A., Mallikarjuna, N.N., Aminabhavi, T.M., 2004. Recent advances on chitosan-based micro- and nanoparticles in drug delivery. J. Control. Release 100, 5–28.

Alemka, A., Corcionivoschi, N., Bourke, B., 2012. Defense and adaptation: the complex inter-relationship between Campylobacter jejuni and mucus. Front. Cell. Infect. Microbiol. 2, 15.

Alemka, A., Nothaft, H., Zheng, J., Szymanski, C.M., 2013. N-glycosylation of Campylobacter jejuni surface proteins promotes bacterial fitness. Infect. Immun. 81, 1674–1682.

Allos, B.M., 2001. Campylobacter jejuni Infections: update on emerging issues and trends. Clin. Infect. Dis. 32, 1201–1206.

Al-Manasir, N., Zhu, K., Kjoniksen, A.L., Knudsen, K.D., Karlsson, G., Nystrom, B., 2009. Effects of temperature and pH on the contraction and aggregation of microgels in aqueous suspensions. J. Phys. Chem. B 113, 11115–11123.

Annamalai, T., Pina-Mimbela, R., Kumar, A., Binjawadagi, B., Liu, Z., Renukaradhya, G.J., Rajashekara, G., 2013. Evaluation of nanoparticle-encapsulated outer membrane proteins for the control of Campylobacter jejuni colonization in chickens. Poult. Sci. 92, 2201–2211.

Arca, H.C., Gunbeyaz, M., Senel, S., 2009. Chitosan-based systems for the delivery of vaccine antigens. Expert Rev. Vaccines 8, 937–953.

Bae, J., Oh, E., Jeon, B., 2014. Enhanced transmission of antibiotic resistance in Campylobacter jejuni biofilms by natural transformation. Antimicrob. Agents Chemother. 58, 7573–7575.

Basler, M., Mekalanos, J.J., 2012. Type 6 secretion dynamics within and between bacterial cells. Science 337, 815.

Basler, M., Pilhofer, M., Henderson, G.P., Jensen, G.J., Mekalanos, J.J., 2012. Type VI secretion requires a dynamic contractile phage tail-like structure. Nature 483, 182–186.

Beery, J.T., Hugdahl, M.B., Doyle, M.P., 1988. Colonization of gastrointestinal tracts of chicks by Campylobacter jejuni. Appl. Environ. Microbiol. 54, 2365–2370.

Bleumink-Pluym, N.M., van Alphen, L.B., Bouwman, L.I., Wosten, M.M., van Putten, J.P., 2013. Identification of a functional type VI secretion system in Campylobacter jejuni conferring capsule polysaccharide sensitive cytotoxicity. PLoS Pathog. 9, e1003393.

Boyer, F., Fichant, G., Berthod, J., Vandenbrouck, Y., Attree, I., 2009. Dissecting the bacterial type VI secretion system by a genome wide in silico analysis: what can be learned from available microbial genomic resources? BMC Genomics 10, 104.

Brown, H.L., Hanman, K., Reuter, M., Betts, R.P., van Vliet, A.H., 2015. Campylobacter jejuni biofilms contain extracellular DNA and are sensitive to DNase I treatment. Front. Microbiol. 6, 699.

Buckley, A.M., Wang, J., Hudson, D.L., Grant, A.J., Jones, M.A., Maskell, D.J., Stevens, M.P., 2010. Evaluation of live-attenuated Salmonella vaccines expressing Campylobacter antigens for control of C. jejuni in poultry. Vaccine 28, 1094–1105.

Burtnick, M.N., Brett, P.J., Harding, S.V., Ngugi, S.A., Ribot, W.J., Chantratita, N., Scorpio, A., Milne, T.S., Dean, R.E., Fritz, D.L., Peacock, S.J., Prior, J.L., Atkins, T.P., Deshazer, D., 2011. The cluster 1 type VI secretion system is a major virulence determinant in Burkholderia pseudomallei. Infect. Immun. 79, 1512–1525.

Chen, W.P., Kuo, T.T., 1993. A simple and rapid method for the preparation of gram-negative bacterial genomic DNA. Nucleic Acids Res. 21, 2260.

Chiang, H.I., Berghman, L.R., Zhou, H., 2009. Inhibition of NF-kB 1 (NF-kBp50) by RNA interference in chicken macrophage HD11 cell line challenged with Salmonellaenteritidis. Genet. Mol. Biol. 32, 507–515.

Chung, Y., Chang, S.H., Martinez, G.J., Yang, X.O., Nurieva, R., Kang, H.S., Ma, L., Watowich, S.S., Jetten, A.M., Tian, Q., Dong, C., 2009. Critical regulation of early Th17 cell differentiation by interleukin-1 signaling. Immunity 30, 576–587.

Clark, J.D., Oakes, R.D., Redhead, K., Crouch, C.F., Francis, M.J., Tomley, F.M., Blake, D.P., 2012. Eimeria species parasites as novel vaccine delivery vectors: anti-Campylobacter jejuni protective immunity induced by Eimeria tenella-delivered CjaA. Vaccine 30, 2683–2688.

Conlan, A.J., Coward, C., Grant, A.J., Maskell, D.J., Gog, J.R., 2007. Campylobacter jejuni colonization and transmission in broiler chickens: a modelling perspective. J. R. Soc. Interface 4, 819–829.

Connell, S., Meade, K.G., Allan, B., Lloyd, A.T., Kenny, E., Cormican, P., Morris, D.W.,

Bradley, D.G., O'Farrelly, C., 2012. Avian resistance to Campylobacter jejuni colonization is associated with an intestinal immunogene expression signature identified by mRNA sequencing. PLoS One 7, e40409.
Corcionivoschi, N., Gundogdu, O., Moran, L., Kelly, C., Scates, P., Stef, L., Cean, A., Wren, B., Dorrell, N., Madden, R.H., 2015. Virulence characteristics of hcp+ Campylobacter jejuni and Campylobacter coli isolates from retail chicken. Gut Pathog. 7, 20.
Davis, L., DiRita, V., 2008. Growth and laboratory maintenance of Campylobacter jejuni. Curr. Protoc. Microbiol Chapter 8, Unit 8A.1.1-8A.1.7.
Davis, L.M., Kakuda, T., DiRita, V.J., 2009. A Campylobacter jejuni znuA orthologue is essential for growth in low-zinc environments and chick colonization. J. Bacteriol. 191, 1631–1640.
Dudley, E.G., Thomson, N.R., Parkhill, J., Morin, N.P., Nataro, J.P., 2006. Proteomic and microarray characterization of the AggR regulon identifies a pheU pathogenicity island in enteroaggregative Escherichia coli. Mol. Microbiol. 61, 1267–1282.
Harrison, J.W., Dung, T.T.N., Siddiqui, F., Korbrisate, S., Bukhari, H., Tra, M.P.V., Hoang, N.V.M., Carrique-Mas, J., Bryant, J., Campbell, J.I., Studholme, D.J., Wren, B.W., Baker, S., Titball, R.W., Champion, O.L., 2014. Identification of possible virulence marker from Campylobacter jejuni isolates. Emerg. Infect. Dis. 20, 1026–1029.
Hendrixson, D.R., DiRita, V.J., 2004. Identification of Campylobacter jejuni genes involved in commensal colonization of the chick gastrointestinal tract. Mol. Microbiol. 52, 471–484.
Hermans, D., Van Deun, K., Messens, W., Martel, A., Van Immerseel, F., Haesebrouck, F., Rasschaert, G., Heyndrickx, M., Pasmans, F., 2011. Campylobacter control in poultry by current intervention measures ineffective: urgent need for intensified fundamental research. Vet. Microbiol. 152, 219–228.
Hermans, D., Pasmans, F., Heyndrickx, M., Van Immerseel, F., Martel, A., Van Deun, K., Haesebrouck, F., 2012. A tolerogenic mucosal immune response leads to persistent Campylobacter jejuni colonization in the chicken gut. Crit. Rev. Microbiol. 38, 17–29.
Hong, Y.H., Lillehoj, H.S., Lee, S.H., Dalloul, R.A., Lillehoj, E.P., 2006. Analysis of chicken cytokine and chemokine gene expression following Eimeria acervulina and Eimeria tenella infections. Vet. Immunol. Immunopathol. 114, 209–223.
Jafarlou, M., Baradaran, B., Shanehbandi, D., Saedi, T.A., Jafarlou, V., Ismail, P., Othman, F., 2016. siRNA-mediated inhibition of survivin gene enhances the anti-cancer effect of etoposide in U-937 acute myeloid leukemia cells. Cell. Mol. Biol. (Noisy-le-grand) 62, 44–49.
Kakuda, T., DiRita, V.J., 2006. Cj1496c encodes a Campylobacter jejuni glycoprotein that influences invasion of human epithelial cells and colonization of the chick gastrointestinal tract. Infect. Immun. 74, 4715–4723.
Kakuda, T., Koide, Y., Sakamoto, A., Takai, S., 2012. Characterization of two putative mechanosensitive channel proteins of Campylobacter jejuni involved in protection against osmotic downshock. Vet. Microbiol. 160, 53–60.
Kamat, V., Marathe, I., Ghormade, V., Bodas, D., Paknikar, K., 2015. Synthesis of monodisperse chitosan nanoparticles and in situ drug loading using active microreactor. ACS Appl. Mater. Interfaces 7, 22839–22847.
Karlyshev, A.V., Everest, P., Linton, D., Cawthraw, S., Newell, D.G., Wren, B.W., 2004. The Campylobacter jejuni general glycosylation system is important for attachment to human epithelial cells and in the colonization of chicks. Microbiology 150, 1957–1964.
Kobierecka, P.A., Olech, B., Ksiazek, M., Derlatka, K., Adamska, I., Majewski, P.M., Jagusztyn-Krynicka, E.K., Wyszynska, A.K., 2016a. Cell Wall Anchoring of the Campylobacter Antigens to Lactococcus lactis. Front. Microbiol. 7, 165.
Kobierecka, P.A., Wyszynska, A.K., Gubernator, J., Kuczkowski, M., Wisniewski, O., Maruszewska, M., Wojtania, A., Derlatka, K.E., Adamska, I., Godlewska, R., Jagusztyn-Krynicka, E.K., 2016b. Chicken anti-campylobacter vaccine - comparison of various carriers and routes of immunization. Front. Microbiol. 7, 740.
Kuskonmaz, B., Yurdakok, K., Yalcin, S.S., Ozmert, E., 2009. Comparison of acute bloody and watery diarrhea: a case control study. Turk. J. Pediatr. 51, 133–140.
Lacharme-Lora, L., Chaloner, G., Gilroy, R., Humphrey, S., Gibbs, K., Jopson, S., Wright, E., Reid, W., Ketley, J., Humphrey, T., Williams, N., Rushton, S., Wigley, P., 2017. B lymphocytes play a limited role in clearance of Campylobacter jejuni from the chicken intestinal tract. Sci. Rep. 7 45090-45090.
Laniewski, P., Kuczkowski, M., Chrzastek, K., Wozniak, A., Wyszynska, A., Wieliczko, A., Jagusztyn-Krynicka, E.K., 2014. Evaluation of the immunogenicity of Campylobacter jejuni CjaA protein delivered by Salmonella enterica sv. Typhimurium strain with regulated delayed attenuation in chickens. World J. Microbiol. Biotechnol. 30, 281–292.
Larsen, J.C., Szymanski, C., Guerry, P., 2004. N-linked protein glycosylation is required for full competence in Campylobacter jejuni 81-176. J. Bacteriol. 186, 6508–6514.
Layton, S.L., Morgan, M.J., Cole, K., Kwon, Y.M., Donoghue, D.J., Hargis, B.M., Pumford, N.R., 2011. Evaluation of Salmonella-vectored Campylobacter peptide epitopes for reduction of Campylobacter jejuni in broiler chickens. Clin. Vaccine Immunol. 18, 449–454.
Leiman, P.G., Basler, M., Ramagopal, U.A., Bonanno, J.B., Sauder, J.M., Pukatzki, S., Burley, S.K., Almo, S.C., Mekalanos, J.J., 2009. Type VI secretion apparatus and phage tail-associated protein complexes share a common evolutionary origin. Proc. Natl. Acad. Sci. U. S. A. 106, 4154–4159.
Lertpiriyapong, K., Gamazon, E.R., Feng, Y., Park, D.S., Pang, J., Botka, G., Graffam, M.E., Ge, Z., Fox, J.G., 2012. Campylobacter jejuni type VI secretion system: roles in adaptation to deoxycholic acid, host cell adherence, invasion, and in vivo colonization. PLoS One 7, e42842.
Li, Y.P., Ingmer, H., Madsen, M., Bang, D.D., 2008. Cytokine responses in primary chicken embryo intestinal cells infected with Campylobacter jejuni strains of human and chicken origin and the expression of bacterial virulence-associated genes. BMC Microbiol. 8, 107.
Lien, Y.W., Lai, E.M., 2017. Type VI secretion effectors: methodologies and biology. Front. Cell. Infect. Microbiol. 7, 254.
Luo, Y., Zhang, B., Cheng, W.-H., Wang, Q., 2010. Preparation, characterization and evaluation of selenite-loaded chitosan/TPP nanoparticles with or without zein coating. Carbohydr. Polym. 82, 942–951.
Maciel, M., Fusaro, A.E., Oliveira, C.R., Futata, E.A., Duarte, A.J.S., Sato, M.N., 2004. IgA response in serum and gut secretion in sensitized mice fed with the dust mite Dermatophagoides pteronyssinus extract. Braz. J. Med. Biol. Res. 37, 817–826.
Macpherson, A.J., Smith, K., 2006. Mesenteric lymph nodes at the center of immune anatomy. J. Exp. Med. 203, 497–500.
Mallick, A.I., Haq, K., Brisbin, J.T., Mian, M.F., Kulkarni, R.R., Sharif, S., 2011. Assessment of bioactivity of a recombinant chicken interferon-gamma expressed using a baculovirus expression system. J. Interferon Cytokine Res. 31, 493–500.
Malmo, J., Varum, K.M., Strand, S.P., 2011. Effect of chitosan chain architecture on gene delivery: comparison of self-branched and linear chitosans. Biomacromolecules 12, 721–729.
Mougous, J.D., Cuff, M.E., Raunser, S., Shen, A., Zhou, M., Gifford, C.A., Goodman, A.L., Joachimiak, G., Ordonez, C.L., Lory, S., Walz, T., Joachimiak, A., Mekalanos, J.J., 2006. A virulence locus of Pseudomonas aeruginosa encodes a protein secretion apparatus. Science 312, 1526–1530.
Murdoch, S.L., Trunk, K., English, G., Fritsch, M.J., Pourkarimi, E., Coulthurst, S.J., 2011. The opportunistic pathogen Serratia marcescens utilizes type VI secretion to target bacterial competitors. J. Bacteriol. 193, 6057–6069.
Neal-McKinney, J.M., Samuelson, D.R., Eucker, T.P., Nissen, M.S., Crespo, R., Konkel, M.E., 2014. Reducing Campylobacter jejuni colonization of poultry via vaccination. PLoS One 9, e114254.
Newell, D.G., Fearnley, C., 2003. Sources of Campylobacter colonization in broiler chickens. Appl. Environ. Microbiol. 69, 4343–4351.
Noreen, Z., Jobichen, C., Abbasi, R., Seetharaman, J., Sivaraman, J., Bokhari, H., 2018. Structural basis for the pathogenesis of Campylobacter jejuni Hcp1, a structural and effector protein of the Type VI Secretion System. FEBS J. 285, 4060–4070.
Nothaft, H., Davis, B., Lock, Y.Y., Perez-Munoz, M.E., Vinogradov, E., Walter, J., Coros, C., Szymanski, C.M., 2016. Engineering the Campylobacter jejuni N-glycan to create an effective chicken vaccine. Sci. Rep. 6, 26511.
Pandey, R., Ahmad, Z., Sharma, S., Khuller, G.K., 2005. Nano-encapsulation of azole antifungals: potential applications to improve oral drug delivery. Int. J. Pharm. 301, 268–276.
Parsons, D.A., Heffron, F., 2005. sciS, an icmF homolog in Salmonella enterica serovar Typhimurium, limits intracellular replication and decreases virulence. Infect. Immun. 73, 4338–4345.
Pawlak, A., Mucha, M., 2003. Thermogravimetric and FTIR studies of chitosan blends. Thermochim. Acta 396, 153–166.
Pei, Z., Burucoa, C., Grignon, B., Baqar, S., Huang, X.Z., Kopecko, D.J., Bourgeois, A.L., Fauchere, J.L., Blaser, M.J., 1998. Mutation in the peb1A locus of Campylobacter jejuni reduces interactions with epithelial cells and intestinal colonization of mice. Infect. Immun. 66, 938–943.
Plapied, L., Vandermeulen, G., Vroman, B., Preat, V., des Rieux, A., 2010. Bioadhesive nanoparticles of fungal chitosan for oral DNA delivery. Int. J. Pharm. 398, 210–218.
Pukatzki, S., Ma, A.T., Sturtevant, D., Krastins, B., Sarracino, D., Nelson, W.C., Heidelberg, J.F., Mekalanos, J.J., 2006. Identification of a conserved bacterial protein secretion system in Vibrio cholerae using the Dictyostelium host model system. Proc. Natl. Acad. Sci. U. S. A. 103, 1528–1533.
Pukatzki, S., McAuley, S.B., Miyata, S.T., 2009. The type VI secretion system: translocation of effectors and effector-domains. Curr. Opin. Microbiol. 12, 11–17.
Radomska, K.A., Vaezirad, M.M., Verstappen, K.M., Wosten, M.M., Wagenaar, J.A., van Putten, J.P., 2016. Chicken immune response after in ovo immunization with chimeric TLR5 activating flagellin of Campylobacter jejuni. PLoS One 11, e0164837.
Rashid, S., Shen, C., Chen, X., Li, S., Chen, Y., Wen, Y., Liu, J., 2015. Enhanced catalytic ability of chitosan–Cu–Fe bimetal complex for the removal of dyes in aqueous solution. RSC Adv. 5, 90731–90741.
Reid, W.D., Close, A.J., Humphrey, S., Chaloner, G., Lacharme-Lora, L., Rothwell, L., Kaiser, P., Williams, N.J., Humphrey, T.J., Wigley, P., Rushton, S.P., 2016. Cytokine responses in birds challenged with the human food-borne pathogen Campylobacter jejuni implies a Th17 response. R. Soc. Open Sci. 3, 150541.
Rice, B.E., Rollins, D.M., Mallinson, E.T., Carr, L., Joseph, S.W., 1997. Campylobacter jejuni in broiler chickens: colonization and humoral immunity following oral vaccination and experimental infection. Vaccine 15, 1922–1932.
Rosenquist, H., Sommer, H.M., Nielsen, N.L., Christensen, B.B., 2006. The effect of slaughter operations on the contamination of chicken carcasses with thermotolerant Campylobacter. Int. J. Food Microbiol. 108, 226–232.
Sahin, O., Morishita, T.Y., Zhang, Q., 2002. Campylobacter colonization in poultry: sources of infection and modes of transmission. Anim. Health Res. Rev. 3, 95–105.
Sahin, O., Luo, N., Huang, S., Zhang, Q., 2003. Effect of Campylobacter-specific maternal antibodies on Campylobacter jejuni colonization in young chickens. Appl. Environ. Microbiol. 69, 5372–5379.
Sainato, R., ElGendy, A., Poly, F., Kuroiwa, J., Guerry, P., Riddle, M.S., Porter, C.K., 2018. Epidemiology of Campylobacter infections among children in Egypt. Am. J. Trop. Med. Hyg. 98, 581–585.
Sawaengsak, C., Mori, Y., Yamanishi, K., Mitrevej, A., Sinchaipanid, N., 2014. Chitosan nanoparticle encapsulated hemagglutinin-split influenza virus mucosal vaccine. AAPS PharmSciTech 15, 317–325.
Sayin, B., Somavarapu, S., Li, X.W., Sesardic, D., Senel, S., Alpar, O.H., 2009. TMC-MCC (N-trimethyl chitosan-mono-N-carboxymethyl chitosan) nanocomplexes for mucosal delivery of vaccines. Eur. J. Pharm. Sci. 38, 362–369.
Schell, M.A., Ulrich, R.L., Ribot, W.J., Brueggemann, E.E., Hines, H.B., Chen, D., Lipscomb, L., Kim, H.S., Mrazek, J., Nierman, W.C., Deshazer, D., 2007. Type VI secretion is a major virulence determinant in Burkholderia mallei. Mol. Microbiol. 64, 1466–1485.

Schrøder, T.D., Long, Y., Olsen, L.F., 2014. Experimental and model study of the formation of chitosan-tripolyphosphate-siRNA nanoparticles. Colloid Polym. Sci. 292, 2869–2880.
Schwarz, S., West, T.E., Boyer, F., Chiang, W.C., Carl, M.A., Hood, R.D., Rohmer, L., Tolker-Nielsen, T., Skerrett, S.J., Mougous, J.D., 2010. Burkholderia type VI secretion systems have distinct roles in eukaryotic and bacterial cell interactions. PLoS Pathog. 6, e1001068.
Scott, N.E., Bogema, D.R., Connolly, A.M., Falconer, L., Djordjevic, S.P., Cordwell, S.J., 2009. Mass spectrometric characterization of the surface-associated 42 kDa lipoprotein JlpA as a glycosylated antigen in strains of Campylobacter jejuni. J. P. Res. 8, 4654–4664.
Silverman, J.M., Brunet, Y.R., Cascales, E., Mougous, J.D., 2012. Structure and regulation of the type VI secretion system. Annu. Rev. Microbiol. 66, 453–472.
Sims, P.A., 2010. Use of a Spreadsheet To Calculate the Net Charge of Peptides and Proteins as a Function of pH: An Alternative to Using "Canned" Programs To Estimate the Isoelectric Point of These Important Biomolecules. J. Chem. Educ. 87, 803–808.
Singh, A., Mallick, A.I., 2019. Role of putative virulence traits of *Campylobacter jejuni* in regulating differential host immune responses. J. Microbiol. 57, 298–309.
Skarp, C.P.A., Hänninen, M.L., Rautelin, H.I.K., 2016. Campylobacteriosis: the role of poultry meat. Clin. Microbiol. Infect. 22, 103–109.
Smith, C.K., Abuoun, M., Cawthraw, S.A., Humphrey, T.J., Rothwell, L., Kaiser, P., Barrow, P.A., Jones, M.A., 2008. Campylobacter colonization of the chicken induces a proinflammatory response in mucosal tissues. FEMS Immunol. Med. Microbiol. 54, 114–121.
Suarez, G., Sierra, J.C., Sha, J., Wang, S., Erova, T.E., Fadl, A.A., Foltz, S.M., Horneman, A.J., Chopra, A.K., 2008. Molecular characterization of a functional type VI secretion system from a clinical isolate of Aeromonas hydrophila. Microb. Pathog. 44, 344–361.
Suarez, G., Sierra, J.C., Kirtley, M.L., Chopra, A.K., 2010. Role of Hcp, a type 6 secretion system effector, of Aeromonas hydrophila in modulating activation of host immune cells. Microbiology 156, 3678–3688.
Suzuki, H., Yamamoto, S., 2009. Campylobacter contamination in retail poultry meats and by-products in the world: a literature survey. J. Vet. Med. Sci. 71, 255–261.
Szymanski, C.M., Burr, D.H., Guerry, P., 2002. Campylobacter protein glycosylation affects host cell interactions. Infect. Immun. 70, 2242.
Theoret, J.R., Cooper, K.K., Zekarias, B., Roland, K.L., Law, B.F., Curtiss 3rd, R., Joens, L.A., 2012. The Campylobacter jejuni Dps homologue is important for in vitro biofilm formation and cecal colonization of poultry and may serve as a protective antigen for vaccination. Clin. Vaccine Immunol. 19, 1426–1431.
Thibodeau, A., Fravalo, P., Perron, A., Lewandowski, S.L., Letellier, A., 2017. Production and characterization of anti-Campylobacter jejuni IgY derived from egg yolks. Acta Vet. Scand. 59, 80.
Vasconcellos, F.C., Goulart, G.A.S., Beppu, M.M., 2011. Production and characterization of chitosan microparticles containing papain for controlled release applications. Powder Technol. 205, 65–70.
Wang, N., Wu, Y., Pang, M., Liu, J., Lu, C., Liu, Y., 2015. Protective efficacy of recombinant hemolysin co-regulated protein (Hcp) of Aeromonas hydrophila in common carp (Cyprinus carpio). Fish Shellfish Immunol. 46, 297–304.
Whitlock, G.C., Deeraksa, A., Qazi, O., Judy, B.M., Taylor, K., Propst, K.L., Duffy, A.J., Johnson, K., Kitto, G.B., Brown, K.A., Dow, S.W., Torres, A.G., Estes, D.M., 2010. Protective response to subunit vaccination against intranasal Burkholderia mallei and B. Pseudomallei challenge. Procedia Vaccinol. 2.
Wu, H.Y., Chung, P.C., Shih, H.W., Wen, S.R., Lai, E.M., 2008. Secretome analysis uncovers an Hcp-family protein secreted via a type VI secretion system in Agrobacterium tumefaciens. J. Bacteriol. 190, 2841–2850.
Wyszynska, A., Raczko, A., Lis, M., Jagusztyn-Krynicka, E.K., 2004. Oral immunization of chickens with avirulent Salmonella vaccine strain carrying C. jejuni 72Dz/92 cjaA gene elicits specific humoral immune response associated with protection against challenge with wild-type Campylobacter. Vaccine 22, 1379–1389.
Yan, S., Gu, W., Xu, Z.P., 2013. Re-considering how particle size and other properties of antigen-adjuvant complexes impact on the immune responses. J. Colloid Interface Sci. 395, 1–10.
Yang, F., Gu, J., Yang, L., Gao, C., Jing, H., Wang, Y., Zeng, H., Zou, Q., Lv, F., Zhang, J., 2017. Protective efficacy of the trivalent Pseudomonas aeruginosa vaccine candidate PcrV-OprI-Hcp1 in murine pneumonia and burn models. Sci. Rep. 7, 3957.
Zhou, Y., Tao, J., Yu, H., Ni, J., Zeng, L., Teng, Q., Kim, K.S., Zhao, G.P., Guo, X., Yao, Y., 2012. Hcp family proteins secreted via the type VI secretion system coordinately regulate Escherichia coli K1 interaction with human brain microvascular endothelial cells. Infect. Immun. 80, 1243–1251.